The fatigue of carbon fibre reinforced plastics - A review

Available online at www.sciencedirect.com

ScienceDirect

Compos B

Composites Part B: Engineering 00 (2019) 1–35

Review Article

The fatigue of carbon fibre reinforced plastics - a review

Parvez Alam[a], Dimitrios Mamalis[a], Colin Robert[a], Christophe Floreani[a], Conchúr M. Ó Brádaigh[a]

[a] *School of Engineering, Institute for Materials and Processes, The University of Edinburgh, UK*

Abstract

Engineering structures are often subjected to the conditions of cyclic-loading, which onsets material fatigue, detrimentally affecting the service-life and damage tolerance of components and joints. Carbon fibre reinforced plastics (CFRP) are high-strength, low-weight composites that are gaining ubiquity in place of metals and glass fibre reinforced plastics (GFRP) not only due to their outstanding strength-to-weight properties, but also because carbon fibres are relatively inert to environmental degradation and as such, show potential as corrosion resistant materials. The effects of cyclic loading on the fatigue of CFRP are detailed in several papers. As such, collating research on CFRP fatigue into a single document is a worthwhile exercise, as it will benefit the engineering-readership interested in designing fatigue resistant structures and components using CFRP. This review article aims to provide the most relevant and up-to-date information on the fatigue of CFRP. The review focuses in particular on defining fatigue and the mechanics of cyclically-loaded composites, elucidating the fatigue response and fatigue properties of CFRP in different forms, discussing the importance of environmental factors on the fatigue performance and service-life, and summarising the different approaches taken to modelling fatigue in CFRP.

Keywords:
A. Carbon fibre, A. Polymer-matrix composites (PMCs), B. Mechanical properties, B. Fatigue

1. Introduction

Carbon fibre reinforced plastics (CFRP) are attractive engineering materials, primarily because they have a high ratio of strength to weight. Their stiffness and strength properties with respect to weight (specific stiffness and specific strength, respectively) are superior to a range of popular engineering materials including polymers, metals/metal alloys and foams. Figure 1 shows a simplified log-log Ashby diagram by which means specific stiffness and strength can be compared [1]. In this figure, the properties of CFRP with respect to weight, are close to the apex of both the abscissa and the ordinate of the Ashby plot. The specific stiffness of CFRP at its highest is ca. 100 MNm/kg, while its specific strength is close to 700 kNm/kg. Technical ceramics are of very high specific stiffness (ca. 400 MNm/kg), though they can have respectable specific strengths to CFRP, they are still only marginally higher than CFRP. Metals and metal alloys have mid-range values if averaged, but they are high density materials and as such are not ideal for low-weight applications.

CFRP can be manufactured in a variety of forms and can be tailored for different applications. Carbon fibres have the added advantage of that they are manufactured in several different forms and from different raw material sources including; PAN (polyacrylonitrile) carbonisation and oil or coal pitch carbonisation. As such, carbon fibres offer a very wide selection of properties to suit an equally wide range of applications. The properties of the individual fibres will depend on the specific manufacturing route undertaken, coupled to its raw material source. Carbon fibres are nevertheless generally categorised according to their tensile strength and modulus properties, Figure 2. In this figure low modulus (LM) carbon fibres tensile modulus values range between 40 and 200 GPa, while their tensile strength values range between 1 and 3.5 GPa, standard modulus (HT) carbon fibres have higher modulus and strength ranges (200-300 GPa and 2.5-5 GPa, respectively), intermediate modulus (IM) carbon fibres have the highest strengths, ranging from 3.5-7 GPa (and ten-

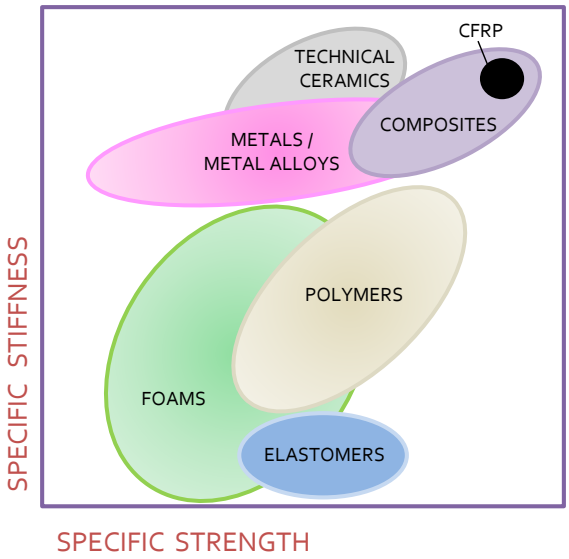

Figure 1. Simplified log-log Ashby diagram showing the specific stiffness against specific strength for different engineering materials.

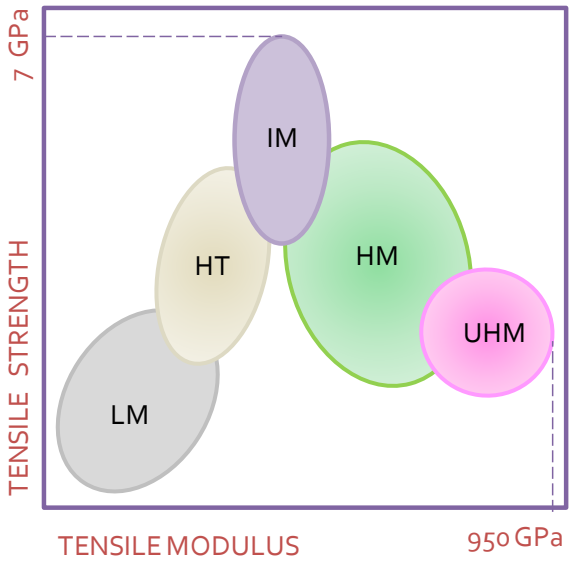

Figure 2. Strength-modulus ranges for different types of carbon fibres graded by their mechanical properties. LM - low modulus, HT - standard modulus, IM - intermediate modulus, HM - high modulus and UHM - ultra high modulus.

sile modulus values between 280-350 GPa), high modulus (HM) carbon fibres exhibit strength ranges that are very similar to HT fibres (though their moduli are higher, 350-600 GPa), and ultra high modulus (UHM) carbon fibres typically do not exceed 4 GPa in strength, but exhibit a range of very high moduli from 600-950 GPa. In composites, the carbon fibres are typically used in long or short filament fibre forms, as chopped or milled fibres, as fibre-mat, as woven fabrics, or as braids.

1.1. Cyclic loading: theory and overview

1.1.1. Fundamentals of fatigue and cyclic loading

Fatigue is the progressive damage of a material when subjected to repeated cyclic loading. Even if a material is loaded at stress levels well below the elastic limit, under the conditions of continuous cyclic loading, microscopic damage occurs. This micro/damage accumulates throughout the material and can grow steadily into macro-cracks, or, may cause macro-scale damage leading to the ultimate failure of the material. Mechanical loading, thermal gradients, chemical ingress and environmental conditions all contribute to the rate at which fatigue damage occurs in materials. As such, fatigue is a complex process as the lifetime of a material under cyclic loading can be affected by many parameters in tandem.

The fatigue life (N) of a component is defined as the total number of stress cycles required to cause material failure. The onset of material failure can be subdivided into distinct stages as shown in Figure 3. In the first stage of fatigue failure; microcracks and open cracks build up within the material. This leads to crack nucleation and minor levels of damage (second stage) which in turn gives rise to damage through micro-cracking (third stage). At this stage, the likelihood of crack nucleation increases as a function of the stress intensity, K_I. Critical factors influencing K_I include topography (of surfaces or interfaces), voids, inclusions and defects. Topographical phenomena such as roughness are important as they are directly related to the intensity and density of existing stress concentrations. Contrarily, smooth surfaces increase the time required for cracks to nucleate. The subsequent stage of fatigue damage is characterised by crack growth, which occurs in a steady manner to a critical size. On reaching a critical size, the crack propagates catastrophically through the material as the remaining materials is unable to sustain any further imposed load.

Figure 3. The different stages of material damage during fatigue.

The most common fatigue testing regimen involves cyclic loading between two predetermined levels of stress. This is termed a constant amplitude stress and is illustrated in Figure 4. The first form of fatigue loading within a constant amplitude stress involves the complete reversal of cycling (tension-compression loading) as is shown in Figure 4(a). Here, the sinusoidal loading wave traverses from a tensile loading mode to a compressive loading mode, the

maximum and minimum stresses being equal. Figure 4(b) depicts repeated cyclic loading (zero-to-tension) where a material carrying no load is subjected to a load, which is subsequently removed such that the material returns to zero-load condition in each cycle. Pure tensile cyclic loading (tension-tension loading) is shown in Figure 4(c) where the stress is tensile during the entire cycle. Figure 4(d) shows random or irregular stress cycling, which is a function of variable amplitudes during loading. This is perhaps the least typical mode of cyclic loading, and yields the least predictable fatigue lifetime of any material.

The stress range, $\Delta\sigma = \sigma_{max} - \sigma_{min}$, is the difference between the maximum and the minimum stresses imposed on a material in fatigue. Averaging the maximum and minimum values results in the mean stress, σ_m. Half the stress range is called the stress amplitude, σ_a, which is essentially the variation about the mean. Mathematical expressions for these basic definitions are: $\sigma_a = \frac{\Delta\sigma}{2} = \frac{\sigma_{max}-\sigma_{min}}{2}$, $\sigma_m = \frac{\sigma_{max}+\sigma_{min}}{2}$. The maximum, σ_{max}, and minimum σ_{min} stress values of the stress amplitude can be expressed as $\sigma_{max} = \sigma_m + \sigma_a$ and $\sigma_{min} = \sigma_m - \sigma_a$. The signs of σ_a and $\Delta\sigma$ are always positive, since $\sigma_{max} > \sigma_{min}$, where tension is considered positive. The quantities σ_{max}, σ_{min} and σ_m can be either positive or negative. Ratios such as the stress ratio R and the amplitude ratio A are commonly used and expressed as: $R = \frac{\sigma_{min}}{\sigma_{max}}$, and $A = \frac{\sigma_a}{\sigma_m}$, respectively. A constant fatigue life (CFL) diagram [4] is usually used to the study the effect of R in the fatigue life of a material. A common procedure involves the use of stress/life information to predict the expected life (or expected stress for a particular probability of failure) of a material by plotting the mean stress against the alternating stress. A widely used illustrative means of estimating the influence of the mean stress on the fatigue strength of a material is through a Goodman diagram [5], Figure 5. This diagram plots stress amplitude against mean stress with the fatigue limit (endurance limit) and the ultimate tensile strength of the material as the two extremes. The Goodman relationship is expressed as $\sigma_a = \sigma_{fat}(1 - \frac{\sigma_m}{\sigma_{uts}})$, where where σ_{fat} is the fatigue limit for completely reversed loading and σ_{uts} is the ultimate tensile strength of the material. The area below the straight line indicates that the material should not fail at given stresses while the area above represents the possibility of failure. Then for any given mean stress, the fatigue (endurance) limit can be evaluated directly as the ordinate of the lifeline at the specific value of σ_m. As the mean stress of a fatigue cycle is increased, the number of cycles to failure and the endurance limit (if existing) decreases. At low stress i.e. high-cycle-fatigue, the fatigue life increases significantly. However, for polymer composites the fatigue mechanism is rather complex and more accurate predictions of the effect of mean stress on fatigue strength are needed. To this effect, a modified Goodman curve proposed by Boller [6] replaces σ_{uts} by the flexural strength of the FRP at a time corresponding to that of the cycle life at the x-axis intercept.

Fatigue analyses are not always based on the stress response, but can also be based on the number of loading cycles needed to create a macro-crack. A distinction can therefore be made between low-cycle fatigue (LCF) and high-cycle fatigue (HCF). LCF relates to loading conditions where the stresses may be high enough to induce irrecoverable damage within the material. The transition from low-cycle fatigue to high-cycle fatigue depends on the properties of the material, but for many materials, it is typically within the range 10^2 to 10^4 cycles [7, 8]. The physical rationale is that in the case of HCF, the stresses are sufficiently low that the material remains within its limit of elastic proportionality. Under LCF, the stress range may surpass this limit of elastic proportionality and as such is more prone to macro-cracking and/or premature failure. As a general rule, when the magnitude of stress is increased, the fatigue life decreases. Fatigue tests are usually represented using an $S-N$ or $\epsilon-N$ diagram, where S is the stress, N is the number of cycles to failure and ϵ is strain. Due to the large variations of N, the abscissa is usually presented in the form of $log(N)$. The $S-N$ curve in the low-cycle fatigue region (Figure 6) is often described by a power law, known as the Coffin-Manson law [2, 3], which is mathematically represented as: $\frac{\Delta\epsilon_p}{2} = \epsilon_f^{'}(2N)^c$ where $\frac{\Delta\epsilon_p}{2}$ is the plastic strain amplitude, $\epsilon_f^{'}$ is an empirical constant (the fatigue ductility coefficient - i.e. the failure strain for a single reversal), $2N$ is the number of reversals to failure (N cycles) and c is an empirical constant (the fatigue ductility exponent). In the high-cycle region of stresses (Figure 6), the elastic component of strain is usually described as the elastic stress amplitude, which follows a power law function of the fatigue life (Basquin law) [9]: $\frac{\Delta\epsilon_e}{2} = \frac{\sigma_f^{'}}{E}(2N)^b$. Here, $\frac{\Delta\epsilon_e}{2}$ is the elastic strain amplitude, $\frac{\sigma_f^{'}}{E}$ is the fatigue strength coefficient and b is a fatigue strength exponent. An important feature is that the fatigue life is expected to increase with an increase of $\sigma_f^{'}$ and a decrease of b. It should be furthermore noted that the fatigue life point ($2N_t$) in the S-N curve transitions as: $2N_t = (\frac{\epsilon_f^{'}E}{\sigma_f^{'}})^{1/b-c}$. The total strain amplitude is the sum of both elastic and plastic strain: $\frac{\Delta\epsilon}{2} = \frac{\Delta\epsilon_p}{2} + \frac{\Delta\epsilon_e}{2}$. It is worth noting that the Coffin-Manson linear damage rule for low cycle fatigue accounts for the plasticity of the material, while Basquin's law is a strain dependent law. If for example, the strain amplitude causes sufficient material plasticity, the lifetime of the material will be short, resulting in an LCF. If however, the stresses are close enough to zero, we can assume that the strains are elastic and as such, that the lifetime of the material will be long (HCF).

1.1.2. Mechanics of cyclically loaded composites

Composites have gained considerable popularity over the last five decades as they can be tailored to have outstanding mechanical, thermal, physical and electrical properties [10, 11, 12, 13, 14]. The fatigue behaviour

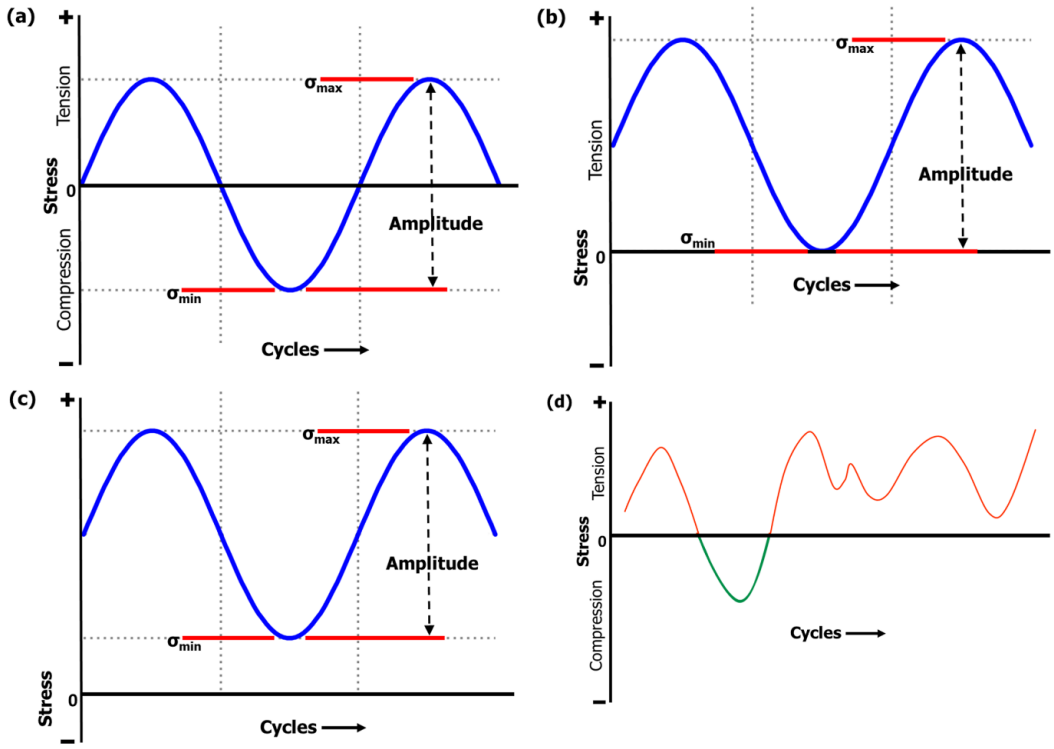

Figure 4. Constant amplitude cycling types: (a) completely reversed cycle of stress (b) repeated cyclic loading (c) purely tensile cycles and (d) random stress cycles.

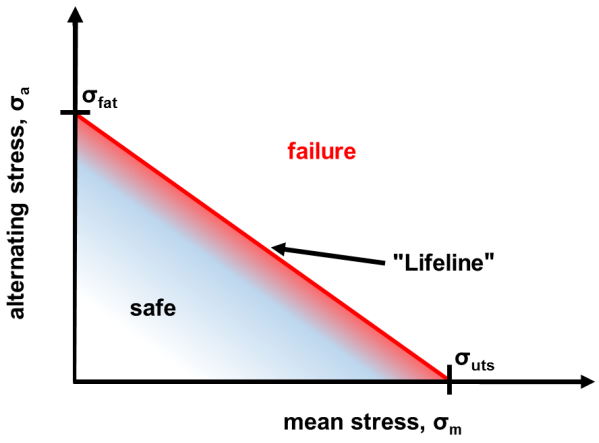

Figure 5. Schematic example of a Goodman diagram.

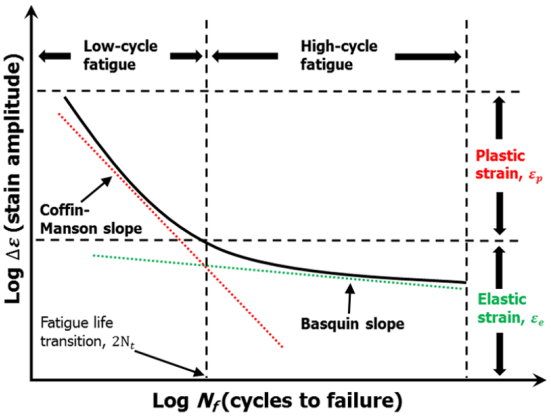

Figure 6. Elastic and plastic strain-life curves to produce total strain-life, ϵ-N, curve of a material.

of composite materials and structures is complex since composites fail by a series of, or collection of damage mechanisms including; fibre breakage, matrix cracking, fibre–matrix debonding, delamination [15] and the effect of shear-induced diffuse damage on transverse cracks [16, 17]. Fibre fracture is highly dependent on fibre strength and matrix cracking can be retarded somewhat, if the reinforced fibres are of high stiffness (such a carbon). This is because high stiffness and strength fibres can endure higher loads, which limits the strain in the system, and thus that of the matrix (under a given load). Debonding can occur if the interface between the fibre and matrix is weakly bonded, which is itself a function of (a) wetting (b) fibre topography and (c) the physical chemistry at fibre-matrix interfaces. If a composite is composed of

multiple layers (ply-laminated) a ply-delamination failure mode may occur through fatigue loading. The fatigue performance of composites is influenced by the composite system itself. Particularly influential parameters include; fibre and matrix properties, lay-up sequence [18, 19], residual stresses due to the manufacturing process or due to discontinuities [20, 21] and the maximum to minimum ratio of stress endured by the material [22, 23, 24, 4], ply orientation [4], the fibre/matrix fractions [25], and environmental conditions affecting the composite components [26, 27, 28]. Exemplary works on the fatigue of composites covered from both experimental [29, 22] and theoretical [4, 30, 31, 32] perspectives may assist in the development of improved methods by which means composite failure can be predicted.

1.2. Objectives

This review aims to familiarise CFRP materials researchers with the latest research on CFRP, cyclic-loading and fatigue. To begin, we will describe the underlying fundamentals of cyclic-loading, how it differs from static loading conditions, and we will follow this with a part on the mechanical theory of fibre reinforced composites subjected to cyclic-loads. We will then proceed with describing fundamental research on the fatigue properties of cyclically-loaded CFRP drawing upon issues such as the effects of fibre volume fraction and dimensions, fibre sizing, fibre orientation and properties. The fatigue properties of CFRP will then be compared against those of other materials, with an aim of drawing benefits and disadvantages in using CFRP for different applications. Since several areas within which CFRP is applied will be subject to extreme temperature variations, submersion and aging, we will continue with a section on the effects of heat, water-ingress and polymer aging on the fatigue properties of CFRP. The different types of damage with respect to different conditions and CFRP types will then be elucidated, after which we will collate the different approaches used to model and predict the fatigue response of CFRP.

2. Cyclically loaded CFRP

2.1. Effect of fibre type on the fatigue life

In the case of composites, where two (or more) constituents are involved the usefulness of an S-N curve may be questioned as the role of each constituent in the fatigue life of the composite needs to be determined individually. Talreja [35], proposed a new framework for the interpretation of fatigue life of composites, where strain and not stress was plotted against the number of cycles thus yielding an $\epsilon-N$ curve (as shown in Figure 9). This was deemed necessary as the composite fatigue limit can be governed to a large extent by the matrix fatigue limit, and that failure at the first cycle occurs when the composite strain equals the failure strain of fibres, irrespective of the fibre volume fraction of the CFRP. The significance of plotting the maximum strain in the first cycle lies in the fact that this strain value provides a good reference point in mapping the extent of damage from the very first cycle, and that subsequent damage (and thus the fatigue life) will depend on this damage state. The three distinctive regions in this $\epsilon - N$ curve (Figure 9) can be associated with different modes of damage. In particular, region-1 represents static-like damage, where the stress applied is high enough to investigate the early onset of fibre breakage. Region-2 is a mid-level state of stress representing fracture initiation and the progressive propagation and coalescence of small-scale cracks to fibres and interfaces. This eventuates in debonding and ultimately, composite failure. Region-3 is the region of no fatigue failure (for a specific number of cycles), located just below the fatigue limit of the matrix where the applied stress is too low to result in crack propagation.

Fibres are the main load bearers in composites and they occupy $30\% - 70\%$ of the total volume. It is expected, for a given type of fibre (e.g. carbon) and a matrix material that the stress-strain relationship alters when the fibre volume fraction and/or the fibre properties in term of stiffness change. Therefore, commercially available carbon fibres with different stiffness and strain failure ranging from ca. 0.5% up to ca. 2.1% can significantly influence the shape of $\epsilon - N$ curve, and consequently, the fatigue life of the composite. The stiffness and failure strain in the fibre direction of a composite are mainly determined by the fibre properties. As described above, region-1 consists of the horizontally extended scatter area related to composite failure strain, ϵ_c. This strain limit is a function of the static strain to failure of the fibres. It worth noting that if the composite failure strain is less than or equal to the matrix strain failure, then region-2 can be omitted. The materials selection of fibres dramatically affects region-2 of the $\epsilon - N$ curve. More specifically, given a same magnitude of fibre strain, HM fibres would experience greater stresses than LM fibres. Hence, lower fatigue degradation is expected in composites containing HM fibres. Considering that fatigue failure cannot occur in composites until cracks are initiated in the matrix, the use of stiffer fibres makes sense in that they can retard crack growth more effectively.

Konur and Matthews [99] detailed the influence of the carbon fibre type (with respect to modulus) on the fatigue properties of UD-CFRP. They summarised the S-N behaviour of composites made from different carbon fibre types; high modulus (HM), high strength (HS) and low modulus (LM), Figure 7. It is clear from the stress-life curves shown in Figure 7, that HM fibres in UD-CFRP are superior in fatigue in view of strength retention as a function of loading cycles [100]. The difference in the damage mechanism between HM, HS and LM fibre UD-CFRP has also been reported [101]. HM UD-CFRP fail catastrophically and in an explosive manner, progressive failure is observed in HS UD-CFRP samples, and LM UD-CFRP failure is stepwise and progressive (more so than HS). The

relationship between fibre stiffness and the failure mode can be explained in terms of the energy stored. Explosive failure occurs because there is a large amount of energy stored and this is released simultaneously once the matrix fractures. Progressive failure, contrarily, is a result of stress localisation and the gradual stepwise release of pockets of stored energy.

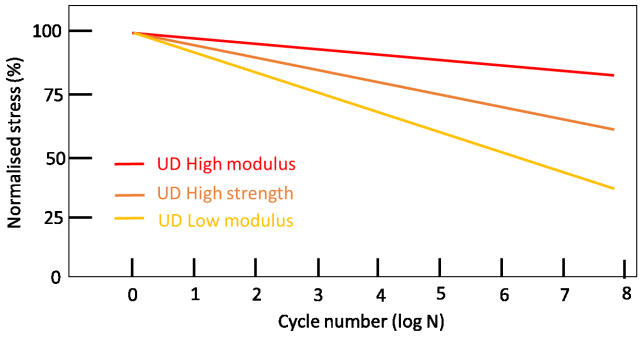

Figure 7. Normalised stress plotted against the number of cycles for different fibre types in T-T fatigue. Figure inspired by the work of [99].

2.2. Thermoset and thermoplastic matrix CFRP

Tai et al. [33] investigated the fatigue behaviour of PEEK based CFRP under tension-tension (T-T) R=0.1, and tension-compression (T-C) R=-0.1 fatigue, using a quasi isotropic-composite configuration. Figure 8 from their paper shows that samples tested in T-C are more sensitive to fatigue loading than the T-T ones. This is understood to be due to the fact that the T-C mode of loading is considerably more damaging to composite materials than T-T [33]. Gamstedt and Talreja [34] compared the fatigue behaviour of CF/epoxy (thermoset resin) to CF/PEEK (thermoplastic resin) composites aligned unidirectionally (R=0.1 T-T at 10 Hz). They noted that the thermoset composite (CF/epoxy) was more resistant to fatigue than CF/PEEK, as only a few microcracks were observed and crack propagation towards the interface was gradual. Contrarily, the thermoplastic composite (CF/PEEK) exhibited widespread debonding, crack propagation and matrix failure. The fatigue life diagrams (FLD) [35] of both CF/epoxy and CF/PEEK UD systems are shown in Figure 9. This leads to a quasi-infinite lifespan, though over time, molecules and interfaces will undoubtedly be affected by the constancy of induced loads and the composite may begin to lose stiffness [34]. Considerably more scatter can be observed in the CF/epoxy composites when compared against the CF/PEEK composites, Figure 10. The properties of CF/PEEK composites nevertheless degrade more swiftly as can be evidenced by the steeper slope in region-2. One reason for why scatter is often noticeably high in fatigue samples could relate to the mechanisms of microdamage. These are essentially related to factors such as defects (which may arise during the manufacturing process), and the homogeneity of the strength of adhesion at fibre-matrix interfaces. When cyclically loaded, microdamage will preferentially initiate from weak spots along fibre matrix interfaces, and in places where defects increase local strain energies. Defects present at interfaces including voids and weakly bonded spots, as well as other defective geometrical arrangements such as fibre misalignment guide the way in which strain energies and stress intensities are distributed (and thus how they propagate) throughout a fatigue loading cycle [39]. By superposing both FLD of CF/epoxy and CF/PEEK UD systems, the authors of [35] inferred that the more ductile PEEK matrix exacerbates the rate at which microscale damage can occur, leading to a more rapid rupture process of fibres, as represented by the steeper slope of region-2. Additionally, region-3 damage, which should be moderate at most, is more prominent in CF/epoxy composites. While the fatigue behaviour is governed by the initiation of cracks and their subsequent development (in the case of CF/epoxy samples), the fatigue properties of CF/PEEK were notably different. In these composites, macroscopic damage is governed by longitudinal splitting, [36]. To better comprehend why there are clear differences between thermoset and thermoplastic matrix CFRPs in fatigue, we will focus on how these different matrices affect crack initiation and development. Comparing the fracture toughness of each is often seen as a good starting point [37]. Hojo et al. investigated the relationships between delamination, fatigue growth and matrix toughness, using PEEK matrix and epoxy matrix CFRPs as archetypal materials of comparison [37]. They found the fracture toughness (static) to be considerably higher in the thermoplastic (PEEK) composites as compared to the thermoset (epoxy) composites. They related this to the higher ductility of the PEEK as compared to the epoxy. Fibres have an additional effect of locally constraining the matrix, which decreases the expanse of plastic zone formation, decreasing thus the rate at which fatigue fractures are able to propagate through the matrix component of composites [38].

2.3. The effects of fibre volume fraction and fibre orientation

The properties of strength and stiffness in composites are usually improved by fibre presence. The fibre volume fraction (FVF) is therefore a critical parameter when considering the fatigue properties of composites. Hiremath et al [40] modelled the effect of fiber volume fraction on damage accumulation within the matrix of an epoxy-matrix CFRP subjected to fatigue stress. They concluded that damage accumulation within the matrix of a composite, decreases as the fibre volume fraction increases. Brunbauer and Pinter [41] conducted an extensive experimental study to discern the effect of mean stress and FVF (30% and 55%) on damage mechanisms in epoxy matrix UD-CFRP. The materials were tested under both static and cyclic conditions in both T-T and T-C modes and oriented

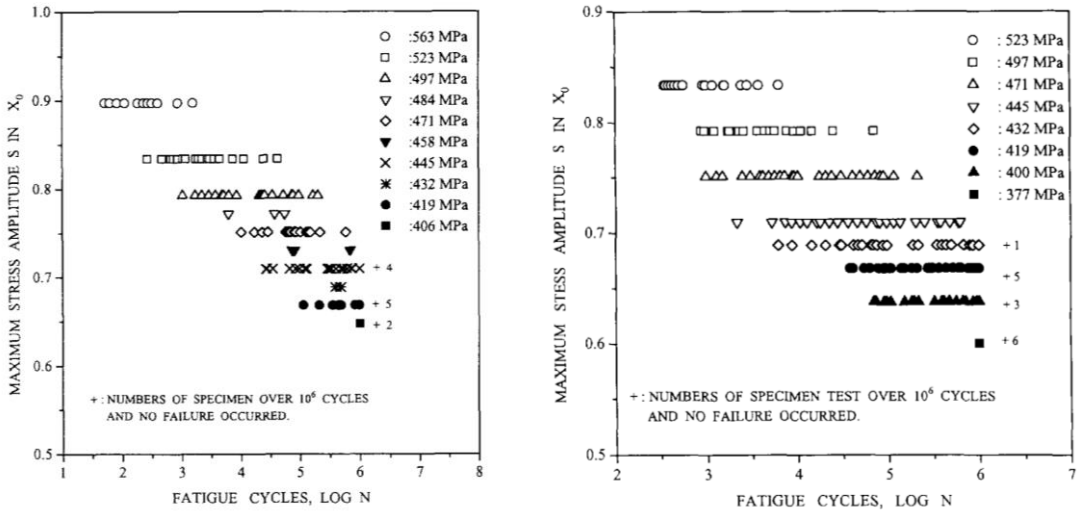

Figure 8. S-N curves of CF/PEEK for T-T (left) and T-C (right) loadings. From [33], reproduced with the permission of Elsevier.

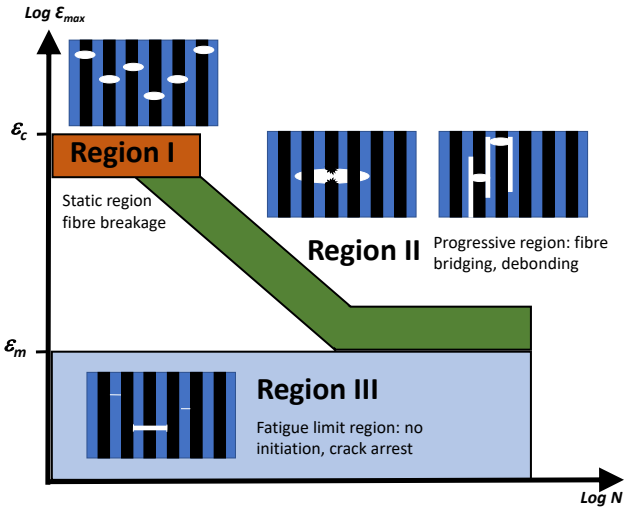

Figure 9. Fatigue life diagram of longitudinal composites in tension-tension fatigue. Figure inspired by the work of [34].

at 0°, 45° and 90°. A schematic summary of their research is provided in Figure 11. The slopes of the S-N curves were steepest for the T-C fatigue tests. Under static loading, a higher FVF (solid lines) resulted in strength improvements in both tension and compression for all fibre orientations. In fatigue, when comparing samples at 30% (dashed lines) and 55% FVF (solid lines), the authors found that the FVF was influential in T-T fatigue over the high cycle fatigue regime for specimens oriented at 90°. The authors postulate that this behaviour is due to a change in the mechanism governing composite damage as it changes from fibre pull-outs at higher stress levels, to matrix failure at lower stress levels (in 30% FVF samples) [42]. In T-C, the S-N trend varies little with respect to FVF. The UD (0°) composite damage mechanisms changed from fibre pull-outs and single fibre fracture in T-T mode, to the breakage of entire fibre bundles in T-C mode. This is deemed to be due to buckling and consecutive fibre bundle breakage initiated by poor stress transfer. The 45° specimens exhibited both matrix failure and fibre pull out damage mechanisms in T-T. In T-C, localised buckling led to fibre-crushing and the breakage of fibre bundles.

2.4. Heat dissipation in CFRP

It is well known that heat affects material deformation under the conditions of long-term loading [43]. During fatigue, heat is produced as a function of material kinematics. The build up of heat in CFRP under cyclic loads is a point of importance as heat can affect the mechanical behaviour, and can also instigate chemical changes to the polymer matrix. Thermography can be used to monitor heat build up in CFRP, [44, 45, 35]. When cyclically loading CFRP under high loads and frequencies, hysteresis loops can be observed to increase in area. This change in hysteresis is due to local stress release and the creation of micro-cracks. Hysteresis loop area is directly correlated to the dissipation of kinetic mechanical energy by the sample. This converts to thermal energy through molecular friction within the material. Higher frequency loads cause greater levels of molecular friction, which in turn results in the release of more heat. Heat within CFRP can accrue over time and is sometimes responsible for premature composite failure. Gornet for example [44], when investigating the influence of stacking sequences (in epoxy matrix CFRP) on self-heating, reported that heat was a cause for early fatigue failure. The temperature elevation was reported as being higher for angle-ply laminates [+45/-45/+45/-45] as compared to cross-ply laminates [0/90/0/90], and greater levels of shearing is the result. This is because the visco-plastic energy released is much higher in proportion

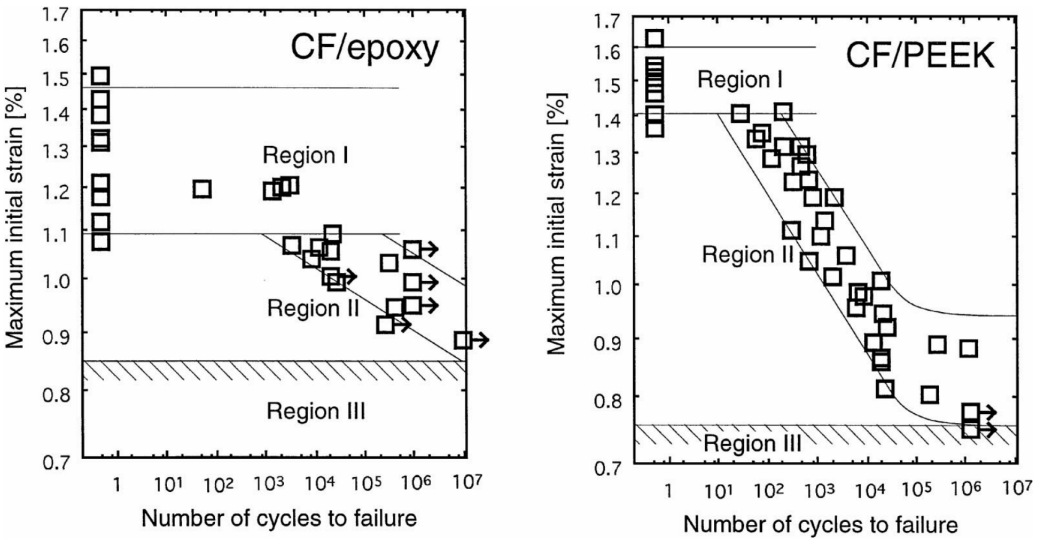

Figure 10. Fatigue life diagram of CF/epoxy and CF/PEEK. Figure from [34], reproduced with the permission of Springer-Nature.

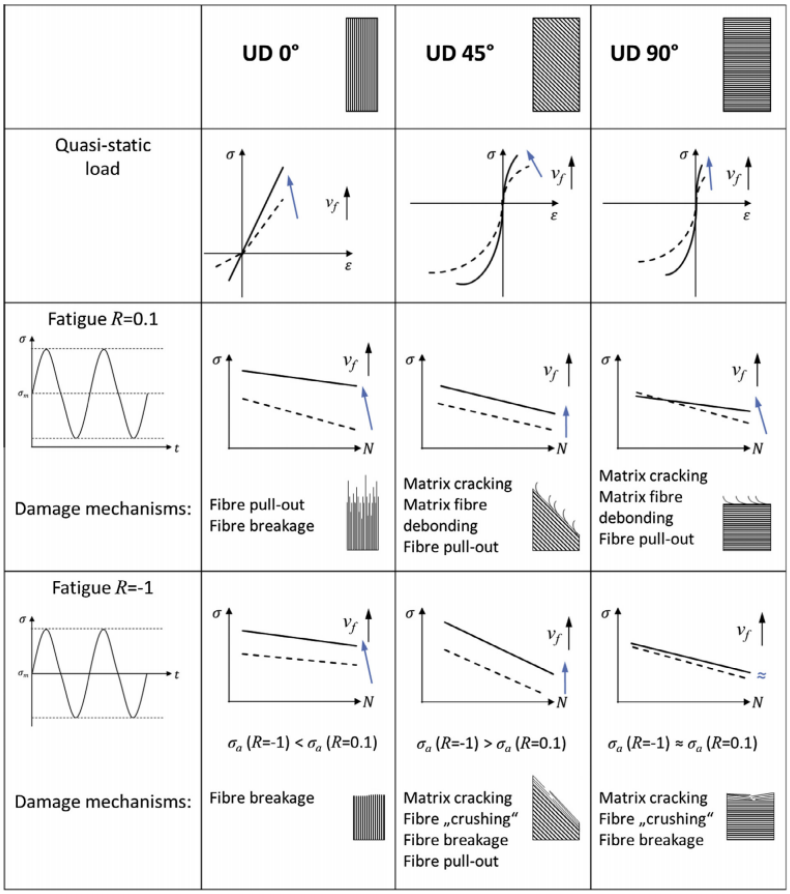

Figure 11. Schematic summary of investigated mechanical behaviour and damage mechanisms in epoxy based UD-CFRP depending of the FVF, the fibres orientation, the fatigue profile (T-T, R=0.1 and T-C, R=-1) and the applied mean stress. From [41], reproduced with the permission of Elsevier.

in angle-ply laminates as compared to cross-ply laminates (Figure 12). The influence of frequency on the fatigue of CFRP is well described through the work of Barron et al. [46]. In their paper, it is noted that kinetic energy generated through fibre-matrix shearing during fatigue, will convert to heat energy within the composite. This heat dissipates between the fibres and matrix primarily through shearing, and for this reason ±45° oriented CFRP are generally more affected by frequency than [0°] oriented (UD) CFRP [46]. ±45° oriented CFRP experience greater magntiudes of deformational shear between fibre and matrix than UD CFRP and as such convert more kinetic energy into heat energy, which in turn reduces the stiffness of the matrix material. At low frequency fatigue, the convection of heat from the sample to air may enable the matrix to stay well below its glass transition temperature. However, under high frequency fatigue more heat is produced within the composite and the temperature of the matrix may rise above its glass transition temperature, which in turn softens the matrix and greatly reduces stress transfer between matrix and fibre, reducing thus the lifespan of the composite [47]. Montesano [48] evidenced that heat production in epoxy matrix CFRP fatigued over 7000 loading cycles is inhomogeneous. The samples were loaded from 40% to 80% of the UTS and an IR (Infra Red) camera used to monitor heat dissipation. At 80% of the UTS, a higher crack density was noted to occur in localised areas, which is presumed to have been the instigator of failure (Figure 13). The self-heating vs fatigue stress study [45] on a PA6.6 matrix CFRP comprising 2 stacking sequences, $[0]_8$ and $[45]_8$, revealed that under higher loading cycles, the temperature of CFRP rises more swiftly and this leads to exacerbated damage (Figure 14). This is because local heat increases the mobility of polymeric chains and reduces the stress transfer between the fibres and matrix, allowing thus, greater straining and more pronounced damage of the CFRP. Interestingly, the stacking sequence is as important in thermoplastic matrix CFRP as it is in thermoset matrix CFRP, $[45]_8$ sequence samples being more affected by heat induced visco-plasticity than $[0]_8$, once again because these composites experience more internal shear.

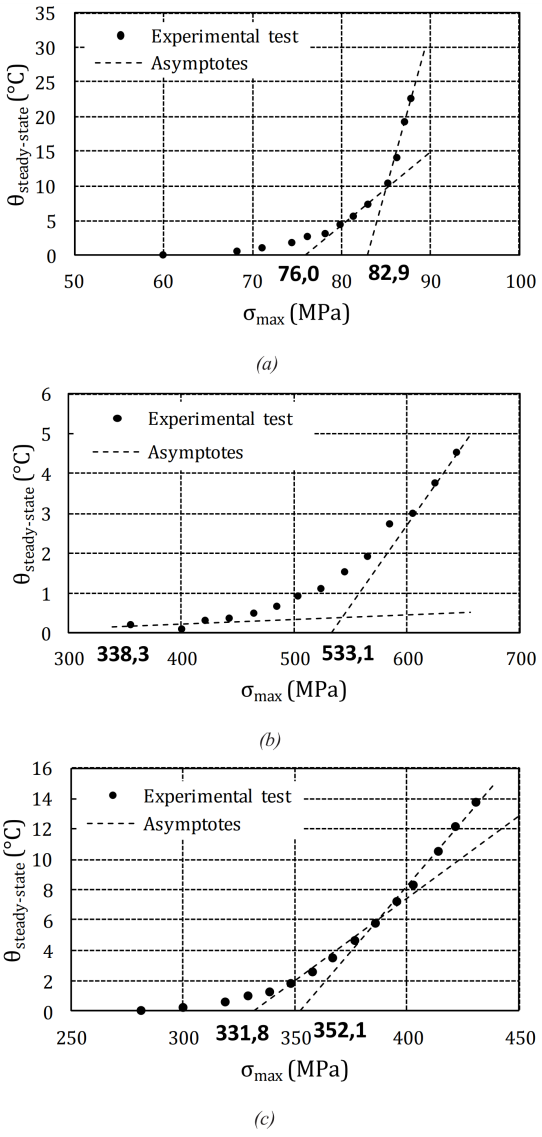

Figure 12. Experimental self-heating curves for epoxy based CFRP (a) $[+45/\text{-}45]_{2s}$, (b) $[0/90]]_{2s}$, (c) $[+45/\text{-}45/90/0]]_s$. From [44], reproduced with the permission of Elsevier.

2.5. The effects of fibre sizing, properties and dimension

The strength of interfacial adhesion can be attributed to; adsorption and wetting, inter-diffusion, electrostatic attraction, chemical bonding, and mechanical adhesion. Interfacial properties affect the fatigue behaviour of CFRP [50]. Good adhesion at the fibre-matrix interface maximises the homogeneity of stress transfer from between the fibres and matrix. Logically fibre sizing, which influences the strength of the interface, will also influence the fatigue lifetime of CFRP. Broyles et al. [51] considered the influence of different types of fibre sizing on the tension-compression fatigue of carbon fibre/vinyl ester UD composites manufactured by resin infusion. Two dissimilar sizing agents were used in the research; poly(vinyl pyrrolidone) (PVP) a brittle thermoplastic, and phenoxy resin (polyhydroxyether) a ductile thermoplastic. Both were compared to unsized CFRP composites and both sizings were shown to have an important effect on the fatigue properties of CFRP. An increase of 60% in the fatigue life was reported when phenoxy sized fibres were used, and an improvement of 20% of the fatigue life reported for the PVP sized fibres. Under similar loading conditions (207 MPa), the lifespan of phenoxy sized CFRP composites was found to be 20 times greater than unsized CFRP composites, Figure 15. Deng et al. [52] reported similar behaviour when researching 0° and 90° UD-CFRP under tension-tension fatigue. In their study, treated carbon fibre pre-preg composites showed an improvement in fa-

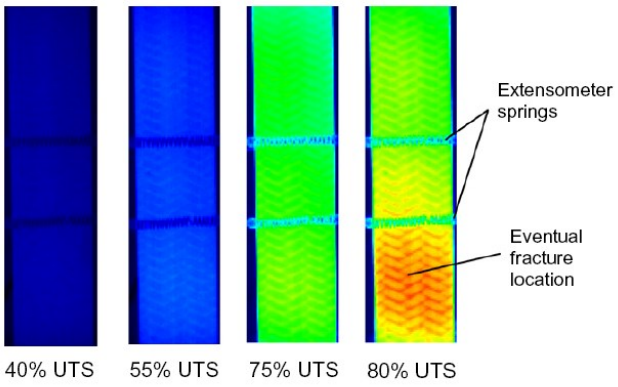

Figure 13. IR temperature distribution after stabilisation for different fatigue stress levels. From [48], reproduced with the permission of Elsevier.

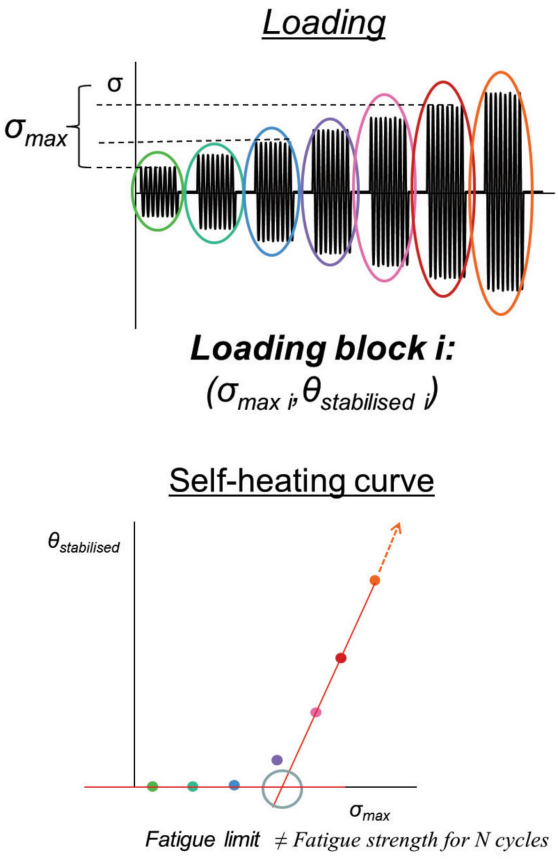

Figure 14. Explanation of fatigue limit detection: block of loading and self-heating curves. From [45], reproduced with the permission of Elsevier.

tigue life when compared to untreated composites under high imposed cyclic stresses. At lower cyclic stresses, fibre treatment was noted to have a reduced effect on the fatigue properties of CFRP.

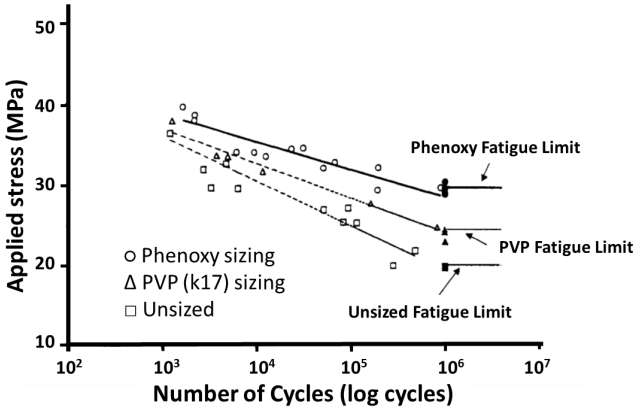

Figure 15. S-N curves of UD carbon fibre/vinyl ester composites with and without sizing in tension-compression. From [51], modified with the permission of Elsevier.

2.6. Short fibre CFRP composites in fatigue

Despite their superior properties, carbon fibres are not usually used as short fibres (unlike glass fibres), since they are more expensive. As such, their target areas are typically higher performance structures where long fibre reinforcements are needed [57]. Fsuchiyama's [53] research on randomly oriented CF (T300S, average diameter = 7 micrometer) focused on the length (in a polyester matrix) revealed that maximum flexural strength of CFRP occurred at a carbon fibre length of 25.4mm. Hitchen et al. [55] further demonstrated that the tensile properties of short fibre epoxy-matrix CFRP were unaffected by the length of carbon fibres up to 5mm within an epoxy matrix. In their work, they found there was a significant reduction of strength from 5mm to 1mm carbon fibre reinforcements. Caprino [54] attributed the difference in the fibre length threshold to both the dissimilar loading modes (T-C vs T-T) and the specific matrices used (polyester vs epoxy). Generally, in static tension, mechanical behaviour is governed by the reinforcement, even though the length of the fibres may be short (up to 3 mm) [54, 55, 56, 57]. Figure 16 shows how the CF aspect ratio influences the fatigue properties of carbon short-fibre reinforced plastics (CSFRP). As the fibres are shortened, load transfer is less effective, which results in the onset of early cracking. A 10,000 fold reduction in the lifespan of CSFRP under similar loading conditions has been reported for 1mm long carbon fibres as compared to 15mm long carbon fibres [49].

In contrast to short fibre reinforced thermosets, short fibre reinforced thermoplastics have received considerable attention [58] since their manufacture through injection molding is suitable for high tonnage, low cost production. Mandell et al. investigated both GSFRP and CSFRP using various thermoplastic matrices, as well as neat PA-66 Nylon, polyamide-imide (PAI), polycarbonate (PC), polyphenylene sulfide (PPS), and polysulfone (PSUL) [59]. CSFRP with brittle matrices are more resilient to high-

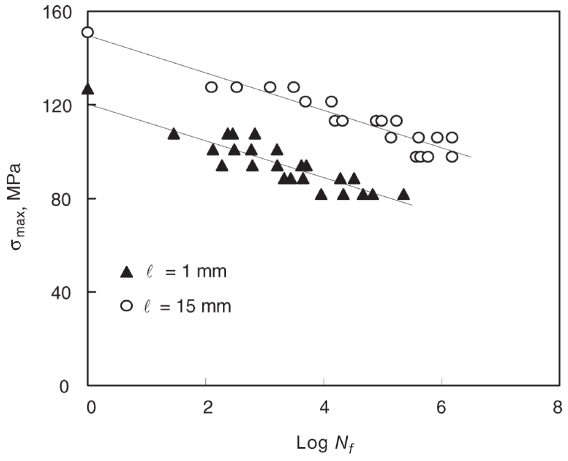

Figure 16. Effect of the fibre length on the S-N curve of random short fibre carbon/epoxy composites. R=0.1. From [54] using data from [55], reproduced with the permission of Elsevier.

cycle fatigue as compared to GSFRP. This tendency is nonetheless, less apparent when more ductile, thermoplastic matrices are used. The authors postulate that the cracked regions are more resilient to fracture in brittle matrix composites than in ductile matrix composites, when subjected to low cycle fatigue. This can be backed up using CSFRP thermosets as an example, as they are far more resilient than CSFRP thermoplastics under high-cycle fatigue. Recent efforts in recycling carbon fibre has renewed a certain interest in the field of CSFRP for structural applications [60], as SFRP are an appropriate material to make from recycled fibres and plastics.

2.7. Effect of processing/manufacturing defects on the fatigue properties

The manufacturing of CFRP is somewhat complex as there are many control parameters that require fine-tuning to improve the final quality of the composite material. To claim that the manufacture of defect-free composites is extremely difficult is by no means an exaggeration. There are manufacturing challenges to be met if the fatiuge properties of CFRP composites are to reach a desirable theoretical level. Types of defects that have been identified as arising through the manufacturing process of CFRP include; voids, curing, environmentally induced defects, and fibre waviness or crimped tows. These are considered amongst the more significant manufacturing induced defects that affect the structural performance and thus, the fatigue life of CFRP [61, 62, 63, 64, 65, 66, 67, 68, 69, 70, 71].

Void formation is possibly the most common manufacturing defect and is inherent to most composite manufacturing techniques including resin-transfer moulding (RTM), sometimes vacuum assisted (VARTM), both of which are well described in the literature [61, 62, 63, 64, 72, 73]. Air entrapment within a composite can occur during the early stages of manufacturing as air bubbles can become trapped in the matrix (as a viscous liquid resin) during the impregnation and consolidation stages, or through poor wetting of the filaments. The resultant formation of voids can detrimentally reduce the intra-laminar and inter-laminar properties of the final composite. Additionally, volatile components or contaminants can create voids by vaporisition during the thermal cycle [74]. In polymer composites, voids have been shown to act as stress concentrators and as a consequence, increase the likelihood of delamination [75, 64, 65, 66, 67, 76, 61, 73], adversely affecting the compressive strength [64, 77, 78], the shear strength [79, 74, 65, 66, 80], the flexural properties [67, 62, 81] and the fatigue properties [82, 83] of the composite. *S-N* curves reveal that voids shorten the fatigue life of a composite, and increases the rate at which the properties of the composite degrade from cycle to cycle (in both T-T and C-C) [83, 84, 81, 69, 85]. A similar degradation of fatigue life has also been reported for unidirectional CFRP cyclically loading in flexure [83, 81].

Curing is a complex thermo-mechanical process with several associated variables that may influence composite performance, both in the long and short terms. During the manufacturing process of CFRP the resin will undergo a curing reaction and it will transform into a solid. This transformation can cause shrinkage of the resin and this in turn introduces internal residual stresses within the composite. Whereas, shrinkage is dependent on the physical properties of the components and their reactions, the creation of residual stresses within a composite are ultimately a function of the duration and temperature of the curing cycle [67, 62]. The correlation between the appearance of high levels of residual stresses and the fatigue performance of composites (CFRPs) has been reported by many [86, 87, 68, 88, 89]. These researchers have found that the fatigue lifetime of CFRP decreases with a higher presence of residual strains within the composite. Other critical factors such as under-curing or over-curing, cure-induced voids as well as thermal degradations due to temperature overshoots, should be taken into account during the manufacture of CFRP [90, 91, 88] as these can also reduce the service life of the composite.

Fibre waviness and crimping are other problematic defects arising through the manufacturing process. These defects affect the quality of consolidation and thence the fatigue life [92, 93, 88, 70, 94, 71]. Out-of-plane waviness affects the static compressive strength and stiffness of composites, and decreases its fatigue life (C-C) [95, 96, 97]. The fatigue life of axially loaded CFRP with induced out-of-plane fibre waviness, gives rise to a severe degradation of the fatigue life properties of CFRP in (T-T) and (C-C) loading [98, 70].

2.8. Effect of pre-existing damage on the fatigue properties

Post-impact damage fatigue can be a critical determinant of the materials selection and design of CFRP components, joints and parts [102]. The fatigue properties offered

by CFRP, if lost through impact damage, may negate the utility of this material in applications where impact and fatigue are inherently coupled. There are various ways in which impact will affect the structural integrity of a composite. This will rely on various factors including; the materials (both fibre and matrix) making up the composite [103, 104], the orientation and configuration of composite laminates [105], the number of laminates, the thickness of laminates [122], and the impacting material: its hardness, mass and velocity at the point of impact.

Nevertheless, there are certain concepts that can be taken as good starting points in the consideration of post-impact fatigue. Following Nettles et al. [107], we can broadly say that there is an implicit relationship between damage size, residual strength in compression and the number of loading cycles to failure in compression. Compression tends to result in more prominent post-impact fatigue damage evolution as compared to tension [108] due to the repeated buckling of the composite encouraging its delamination behaviour at the site of impact-damage [112]. Cantwell et al [108] researched epoxy matrix CFRP laid up as $[+45, -45, 0, 0, -45, +45, 0, 0]_s$ using both non-woven and mixed-woven layers, and found that the residual tensile strength of post-impact fatigued CFRP actually improved, whereas in compression it decreased. The effect was more apparent in non-wovens and less so in mixed-woven CFRP. Since they also noted that the majority of damage occurred between $[+/-45]$ laminates, much of the resistance to loading post-impact, falls upon the [0] oriented laminates, which are inherently suited to tensile resistance over compressive resistance as they are geometrically unstable in compression, while have optimal stress transfer in tension. The constant life model $a = f(1-m)^u(c+m)^v$ predicts the alternating stress as a function of the mean stress for composites in fatigue. Here, a is the normalised alternating stress, m is the normalised mean stress, c is the normalised compressive strength, the exponents u and v characterise the shape of the tensile and compressive wings of the bell curve, and f is a function of the composite laminate tensile strength. In post-impact fatigue, this model reveals a distinct shift in the shape of the compressive part of the bell curve, further clarifying the importance in defining the type of loading that a composite will experience [110]. Certainly, it would seem that compression-compression fatigue is the most damaging to post-impacted composites. Comparing post impact damaged composites under tension-compression (T-C) and compression-compression (C-C) fatigue, Mitrovic and co-workers reported almost no difference in T-C damage mode between the undamaged and impact-damaged composites, whereas C-C fatigue of impact-damaged composites at high stress levels (70-80%) revealed extensive damage evolution [111]. Melin and Schon [112] further stipulated the post-impact crack line follows the buckle in the CFRP material during compressive fatigue, while Ogasawara and co-workers [113] (using high strength T800S/3900-2B epoxy matrix CFRP) reported that in thick (32 ply) quasi-isotropic laminates $[+45, 0, -45, +90, 0, 0]_{4s}$, that post-impact compressive fatigue advances damage, but primarily within the boundaries of the impact-damaged region.

Cantwell and co-workers [108] also found that fibre architecture had a dramatic impact on the evolution of post-impact damage during fatigue. More specifically, they reported that mixed-wovens exhibited less post-impact damage evolution as compared to non-wovens, which displayed a considerable growth from the original damaged region during fatigue. Saito and Kimpara [114] researching multi-axial stiched CFRP (VARTM manufactured) concluded that the meeting of post-impact transverse cracks with cracks propagating during fatigue, gives rise to stress relaxation in the composite. Stress relaxation is particularly important when environmental factors such as water and temperature, influence CFRP during post-impact fatigue [115, 116]. The impact damaged area allows water to ingress more effectively by creating open areas for water to wick along fibre-matrix interfaces, and moreover increases the area available for water diffusion. In both cases, the impact area becomes more compliant and this coupled with stress relaxation through interconnecting cracks during fatigue, results in considerably reduced capacity for post-impact fatigue load-bearing, with larger variances between dry and wet reported in multi-axial (T700S-12K, VARTM) over plain-woven (T300B-3K, VARTM) composites [115].

The type of material used to make up the composite also plays a critical role in the growth and propagation of post-impact damage. Uda and co-workers [117] for example, report that impact induced delaminations are greater in epoxy matrix CFRP (UT500/Epoxy) than they are in thermoplastic matrix CFRP (AS4/PEEK). This is presumably due to the greater polymer compliance in thermoplastics as compared to highly cross-linked thermosets. This is one of the primary reasons for why thermoplastic phases are considered judicious additions to thermoset matrix CFRPs as a means to improving their impact and post-impact performance [103]. Multi-wall carbon nanotubes (CNT) are also considered a means to redistribution of impact/post-impact energies within a composite and have been detailed by [118]. Using quasi-isotropic $[0, +45, 90, -45]_{2s}$ CFRP laminates, they reported a marginally higher load bearing capacity for CNT infused CFRP over a compression-compression (R=10 at 10Hz) fatigue life, though it might be less industrially applicable once the CNT costs are taken into consideration.

Gemometrical parameters [119], alongside material and loading parameters are also necessary considerations in post-impact fatigue analyses. The energy of impact can have a critical effect on the fatigue life of a composite. Symons and Davis [120] report a decade decrease in the fatigue life of T300/914 quasi-isotropic layup carbon fibre/epoxy when impact pre-fatigue impact energies were increased from 5J to 10J (T-C cycling at $R = -1$). Im-

portantly, they note only slight variations in the damping ratio, Δ between 0.65 and 0.7 for their composites between 10 cycles and 65,500 cycles. This indicates that these composites retain much of their brittle character throughout the entire loading cycle. The damping ratio here is calculated as $\Delta = \frac{u_a}{u_m}$ where u_a is the energy absorbed per cycle, $u_a = \int \sigma d\epsilon$, and u_m is the maximum strain energy stored per cycle, $u_m = \frac{1}{2}\sigma_{max}\epsilon_{max} + \frac{1}{2}\sigma_{min}\epsilon_{min}$. Symons and Davis work also reports considerable post-impact damage evolution under fully reversed T-C cycling, more prominently in the case of higher pre-fatigue impact energy. This is a different outcome to that reported by Mitrovic et. al. [111] who researched considerably lower energy impacts (up to ca. 2J) and clarifies thus, the importance of recognising the extent of impact damage prior to fatigue on damage evolution. Higher velocity impacts, and thus impact energies, will cause more damage composites [121]. Altering the geometries of impacted/fatigued materials can of course alter the extent to which a projectile will cause damage. Tai et al. [122] for example, studying quasi-isotropic T300/976 carbon/epoxy composites, report that stiffness losses in T-T post-impact fatigue are alleviated by increasing the composite thickness. This in turn increases material costs and weight, which is unhelpful when weight saving is a primary goal in using CFRP.

2.9. Effect of fibre architecture on the fatigue properties - 2D CFRP composites

The use of UD laminates is not practical in a plethora of real-world engineering composite structures. Textile composites offer higher drapability [123], which is needed in the manufacture of curved structures. Textiles also are also easier to handle, are consequently less laborious to work with, and automation with this material is fairly well established, resulting in high volumes of production. Textile composites also possess higher interlaminar fracture toughness properties than straight fibre composites. However, the fibre waviness in textiles leads to the development of localised stress concentrations on loading. In the case of woven composites, the static tensile strength and Young's modulus is 15-25% and 20%, respectively, when compared against equivalent fibre-dominated UD composites [124]. Contrarily when the composite layups are matrix-dominated the modulus does not reduce and there is in fact anobserved increase of 10-15% in the static tensile strength when compared to UD composites[124]. This is due to fibre-overlap, which reduces in-plane shear deformations and delamination. In compression, the presence of crimp in textile fibres encourages the formation of kink bands, leading to a reduction in static strength when compared against equivalent UD composites[125].

The fatigue response and damage mechanisms observed in textile composites are different to those of UD composites. In woven composites tested in on-axis (T-T) fatigue [126, 127, 128], cracks first develop in the weft yarns, perpendicular to the loading direction. As these cracks grow, breakage of isolated axial fibres occurs, followed by meta-delaminations (i.e. decohesion of warp and weft fibre bundles), which eventually join at ply boundaries to form interlaminar delaminations. Final failure occurs abruptly when large numbers of axial fibres break at the same time. In the case of (T-C) fatigue [124, 126, 128], delaminations and transverse cracks develop simultaneously, making fibre bundles weaker against buckling. Final failure tends to occur during the compression load of the (T-C) fatigue cycle [128]. This is because the fibre bundles in external plies buckle from a lack of adjacent ply support, while internal plies experience fibre bundle kinking, which in turn leads to final failure. These mechanisms lead to out of plane deformations and accelerates damage propagation in (T-C) fatigue as compared to (T-T) fatigue. This is evidenced by the steeper S-N curve observed in (T-C) fatigue [124]. Very little has been reported on the off-axis fatigue testing of woven composites [124, 129, 130]. Nonetheless, it has been shown in 45° bias fatigue, that damage initiates in the composites through matrix cracking in resin rich regions [124]. This is followed by the formation of meta-delaminations, which subsequently coalesce, and lead to relative displacements between warp and weft bundles. The final failure is caused by bulk delamination between the warp and weft bundles. Matrix dominated damage leads to very high strains to failure (up to 20%) [130]. Kawai et al. [129] compared the fatigue properties of plain woven carbon/epoxy laminates at 0°,15°, 30° and 45° from the warp fibre direction. The on-axis testing exhibits a straight line on a log-log S-N curve up to 10^6 cycles, and shows no apparent fatigue limit to within that number of cycles. Off-axis laminates exhibit an S shape on a log-log S-N plot with an increase in slope in the intermediate range of fatigue life (10^4 cycles), which shows a greater sensitivity to fatigue than the on-axis tested composites. However, in the high cycle range ($> 10^4$ cycles), the S-N curve flattens, demonstrating the existence of a fatigue limit. Cracks in woven composites can arise in the weft direction even at just 10% of tensile strength [131]. The fatigue failure mechanisms of woven composites are highly complex as they vary depending not only on the type of loading and direction, but also on the layup.

Knitted composites are an alternative to woven composites as they have enhanced drapability and a higher impact resistance when compared against other textile-based composites. They can also allow the manufacturing of composites with certain features such as holes already incorporated whilst maintaining continuous fibres. However, very few papers can be found in the literature where their fatigue properties are researched. Pandita et al. [132] compared the fatigue properties of plain woven and knitted fabric composites under (T-T) fatigue. Initial failure occurs in the form of bundle debonds. In the locations where the fibres are off-axis to the loading direction, the meta-delaminations were the damage modes that were found to propagate fastest. This leads to a realignment of the fibres and hence a slower subsequent growth of the debond.

In some cases the debond jumped between two fibre bundles creating continuous matrix cracks. The final failure occurred through fibre pull out. When the S-N curves were normalised by the ultimate tensile stress, the knitted composites were shown to perform similarly to woven laminates in the on-axis direction, though much better in the bias (45°) direction. A stiffness reduction of around 10% was observed for knitted composites regardless of the loading direction, which was similar to that observed for the on-axis woven specimen, but was much lower than the 50% degradation observed during the 45° off-axis plain woven fatigue test. The same trend was observed for the residual strength during fatigue.

Similar to knitted composites, very little literature can be found on the fatigue properties of braided composites. Three different braid angles (25°, 30° and 45°) were studied by Kelkar et al. [133, 134]. They reported that the strength and stiffness of braided laminates decreases as a function of increasing braid angle. Yet, the fatigue properties (normalised by the ultimate tensile strength) were also noted to as being independent of the braid angle. A high endurance limit of 40-50% of the utlimate tensile strength was found, although only one million loading cycles were applied and as such, a fatigue test with a higher number of cycles would need to be carried out to confirm that this represents a fatigue limit. A sudden final failure mode, with no visible cracks or delamination of the plies was observed which would be problematic as it would be difficult to detect damage progression. Montesano et al. [135] studied the fatigue of triaxially braided polyimide composites at room temperature and at 225°C. They found that although the static properties are not really impacted by the temperature increase, there is a reduction in fatigue life at elevated temperatures. Even though the higher temperature led to matrix softening (thus mitigating the initial dominant damage mechanism of braided yarn cracking), the crack density of the composite was noticeably higher at the elevated temperature, leading to a shorter lifetime.

2.10. Effect of fibre architecture on the fatigue properties - 3D CFRP composites

Composite mechanical properties are usually tailored in 2D via stacking sequences, depending on the properties required by creating the structure (e.g. shear: ±45°, longitudinal: UD 0°, uniform: quasi-isotropic). Nevertheless, 2D reinforced composites are prone to delamination due to relatively poor interlaminar properties. This is especially true in fatigue. 3D composites may be used to tackle this intrinsic weakness of 2D composites [136, 137]. Industrially, the use of a 3D preform greatly simplifies the out-of-autoclave (RTM) manufacturing cycle, saving time and money [138]. A through-thickness fibre reinforcement, such as 3D woven, stitched, tufted, z-anchor or z-pinned, as referenced by Mouritz [139], improves considerably, the interlaminar fracture toughness [140], the damage tolerance, the impact resistance, and it limits the propagation of macro-delaminations [141] as compared to 2D material. However, the in-plane properties of composites are lower than those of straight fibre engineering composites. An extensive study of Mouritz and Cox [142] for example, reveals a loss of modulus and strength in quasi static tension, bending, and compression of 3D composites as compared to their 2D counterparts. A loss in the fatigue strength and fatigue life has also been reported [142] in many cases, with some notable exceptions, e.g. Aymerich and Priolo working with [02/90]s graphite based CFRP with Kevlar z-reinforcement in (T-T) fatigue [143]. Mouritz and Cox claims that, if the initial monotonic strength difference is discarded by normalising the S-N curves, the trend is then similar in some cases. This so called, knockdown-behaviour, was demonstrated in compression for a $[0, 90]_s$ stitched CFRP [144], as well as for $[\pm 30,\ 90]_s$ flexure z-pinned CFRP [145]. Exceptions can be noted, such as $[+45/-45/0/90]_s$ quasi-isotropic stitched CFRP in tension [144], where stitched composites performed better at high normalised fatigue stresses, and unidirectional (UD) z-pinned CFRP in tension, where the normalised fatigue life was decreased by increasing the pin content and diameter [146].

As expected, the fatigue properties of 3D composites differs from 2D composites and this depends on several parameters, one of which is the type of reinforcement used in the z-direction. In this section, we will focus on each of the following reinforcement types: 3D woven, 3D stitched, z-pinned and 3D braided.

3D woven composites are standard fabrics with fibres running in the x-(warp) and y-(weft) in-plane directions, with a z-yarn binding the fabric layers. There are two main types of 3D woven composites: interlock fabric, where the z-binder is interlaced with the in-plane yarns, and orthogonal fabric, where the z-binder holds in place the entire stack of 2D fabrics, thus avoiding crimp and maximising the in-plane stiffness [139]. Carvelli et al. [147] showed that there is a dependency of these composites on the loading direction (when comparing 2D and 3D wovens) $[0, 90]_s$ orthogonal CFRP in both warp and weft directions and tested in (T-T) fatigue. The fatigue performance of the 2D samples were in between weft (lower) and warp (higher), although the difference was marginal, especially when considering the propensity for scatter when it comes to fatigue of CFRP. Rudov-Clark and Mouritz investigated the influence of volume content of z-binder yarns on the fatigue properties of 3D orthogonal woven CFRP in (T-T) [148]. Adding z-binder reduced the normalised load cycles-to-failure, which indicates that the 2D CFRP composites have better fatigue properties. They postulate that this deterioration was caused by the fibre arrangement, the formation of resin-rich channels, and through fibre damage due to the weaving process.

3D Stitched fabrics are manufactured by sewing a yarn through multiple 2D fabrics layers. Sewing methods vary from the use of simple orthogonal needles to robotic machines with needles working at different angles simultaneously [149]. The microstructures created by the stitch-

ing process influence the monotonic mechanical properties, and the final 3D stitched composites sometimes display better, sometimes worse moduli and failure strengths as compared to 2D composites [139, 142, 149, 150]. There is nevertheless, little doubt that the delamination toughness [151] and impact resistance [152] always improve through stitching. In fatigue, stitching can be beneficial [143], detrimental [142] or neither beneficial nor detrimental, depending on the influence of the stitch on properties such as stiffness and strength. In 3D woven composites, resin rich regions close to the stitches introduce weak spots in the composites. The fatigue properties are also influenced by fibre related issues intrinsic to the manufacturing route such as tow waviness, crimping and fibre damage/breakage [153]. In (C-C) fatigue, the misalignment of tows accelerates micro-buckling and kinking [154], thereby reducing the fatigue life of stitched 3D composites. In (T-T) fatigue, tow waviness and fibre damage/fracture is responsible for a reduced fatigue life. In both cases of (T-T) and (C-C) fatigue, the initial in-plane strength to failure and stiffness knockdown from the original 2D composites contributes to the shortened fatigue life of 3D stitched fabrics.

Z-pinned composites are stacked 2D fabrics or prepreg laminates reinforced through-thickness using thin rods called z-pins, made of extruded metal or pultruded fibrous composites. The most common way of inserting the pins is by use of an ultrasonic device [155]. The z-pinning of CFRP either decreases, or has no effect on the fatigue life in both (T-T) and (C-C) fatigue [145, 146, 156, 157]. Increasing the pin content and diameter beyond a critical threshold does however reduce the fatigue life [146], the threshold being specific to the CFRP system pinned. As for the other 3D CFRP through-thickness reinforcements, the z-pins cause crimping, misalignment and breaking of the fibres. Carbon fibre distortion and crimping encourages microbuckling in (C-C) fatigue [142, 156], while waviness and fibre breakage reduces the (T-T) fatigue strength [145, 146].

3D braided composites processing technologies are fairly complex and can be grouped into three categories: 3D braided fabrics, 3D axial-braided fabrics, multiaxis 3D braided fabrics, as reported in Bilisik review [158]. From a mechanical standpoint, 3D braided CFRP are serious competitors as they exhibit high stiffness, strength energy absorption and fatigue properties [159]. Furthermore, 3D braided CFRP are flexible, allowing for the easier manufacture of complex parts (near-net-shape) than standard CFRP counterparts [137]. Quasi static tests in tension display an initial stiffening effect due possibly to changes in crystalline orientations [160] and local fibre orientations in the loading direction [159], before softening occurs due through the accumulation of damage. Carvelli et al. [161] compared the normalised S-N curves of UD-CFRP with 3D braided CFRP in (T-T). The results from their study are significant, as they show that 3D braided CFRP is the only CFRP architecture with properties improved upon those of standard UD-CFRP. 3D non-crimp woven and non-crimp stitched are similar to standard UD-CFRP under low cycle fatigue, but are inferior under high cycle fatigue [159].

2.11. Effect of open holes and notches on the fatigue properties of CFRP

As understood from the previous section, the fatigue properties of 3D composites are inferior to equivalent 2D composites. This is due to a knockdown in the in-plane mechanical properties and extra premature failures arising from imperfections within the composite architecture. Nevertheless, when delamination is a primary mode of failure, stitches, pins and z-yarns do in fact, slow down the propagation of cracks that are initiated from edge delaminations [144, 154]. This also improves the fracture toughness [140, 162], and can extend the fatigue life of 3D composites. Composites have a higher propensity towards delamination when they have from macroscopic defects [163]. Therefore notched, lap jointed and open hole composites can actually benefit from such z-direction reinforcements [164].

Bolted joints are an effective way of mechanically connecting composite parts [165]. The circular shape of bolts can be beneficial in delocalising stresses. Driled holes are macro-defects and can reduce the ultimate strength of a composite by ca. 50%, depending on the stacking sequence [166]. Indeed, open hole CFRP are more prone to cracking through delamination and as such, improving the through-thickness performance of CFRP is recognisably important. Undamaged 3D CFRP, though weaker than undamaged UD CFRP, has a better resistance to macro-delamination (as described above) and this results in the improved fatigue performance of 3D composites over UD composites when the samples contain macro-defects such as open holes (3D woven [167] or stitched [168]) and notches [169, 170], with normalised S-N curves. One notable exception can be found in Tsai et al. [171] who showed that the superposition of normalised S-N curves for notched and unnotched samples of 3D woven CFRP were almost identical. Initially cut fibres (ICF) CFRP have been recently scrutinised by the composite community due their unique ability to form complex shapes while retaining excellent mechanical properties, close to those of continuous fibre laminates. As complex structures are often required in the industry, new composite manufacturing routes have to be developed and properties have to be examined. Sudarsono et al. [172] investigated the influence of open holes on the fatigue performance of quasi isotropic ICF CFRP manufactured in autoclave (ICF-A) and through press moulding (ICF-P), and compared against standard CFRP (continuous fibre). They reported that the fatigue strength of ICF-P was about 20% that of the ICF-A, and was slightly higher than that of the continuous CFRP. One way of avoiding macro-damage through bolting is to co-cure structures, thereby creating composite joints. Although the mechanical properties of bolted structures are usually superior to those of joints, the one shot curing of large structures can be an

economical advantage (e.g. in renewable energy turbine blade technologies) [173].

3. Environmental effects on the fatigue performance of CFRP

As has been previously mentioned, CFRP is a material of choice that is gaining ubiquity in several industrial sectors including in transportation, renewable energy and construction. Its fatigue durability will nevertheless be affected by environmental factors, which may be more or less extreme depending on where it is applied. When used in fixed-wing aircraft for example, CFRP can be subjected to extreme variations in temperature ranging from ca. -55°C when cruising at altitudes of 7-10 km up to +30-50°C if landing or remaining stationary in e.g. equatorial countries. CFRP used e.g. tidal blades are in submerged conditions where water ingress into the bulk of the material is inevitable. Additionally, there are pressure fluctuations that affect submerged blades and these will collectively affect the mechanical integrity of CFRP [174]. If CFRP is used over its service-life, which in tidal blades should be 20-25 years, then there will be a degree of aging that affects the composite properties, which is important to factor into life-time predictions as polymer aging weakens a composite and alters its molecular structure, making it more prone to interatomic peeling modes of failure, otherwise known as fast-fracture. The following sections highlight the effects that different environments and conditions have on the mechanical and fatigue performance of CFRP.

3.1. Effects of temperature on CFRP and fatigue

Environmental temperatures tend to affect the bulk of the polymer matrix, and the interfaces of CFRP, more so than the fibres themselves. Carbon fibres begin the process of decomposition at ca. 300°C, which is usually far beyond its utility temperatures when embedded in a polymer matrix to form CFRP. Using PAN based fibres, Sauder and co-workers [175] report the stiffness of carbon fibre as being still above 90% of its original value at temperatures of 1600°C (remaining almost unaffected below temperatures of 1000°C), whereas the strength of the fibres actually increased to an apical value of 2850 MPa at 1800°C, after which it decreased to a room temperature value at 2000°C. In further testing on a rayon-based carbon fibre, they found the same behaviour to be true, though Sauder and co-workers were unable to elucidate a mechanism-based reason for this phenomenon. It is possible that this phenomenon is implicitly linked to the initial heat treatment temperature (HTT) of the carbon fibres, as this has been shown to alter the thermal conductivity of the fibres at different temperatures ranging from 500-2500 K [176]. Under reduced temperatures, carbon fibres retain their resilience and unlike polymers, tend not to become more brittle. Polymers are affected by changes in temperature, becoming softer under higher temperatures and more rigid and brittle at lower temperatures. As such, it is the polymer component (and its interface with fibres) that limits the thermomechanical effectiveness of CFRP.

Temperature cycling affects the physical continuum of a CFRP composite. Cycling the ambient temperature around epoxy matrix CFRP between ca. -50°C and 150°C, causes the growth of micro-cracking parallel to the fibre axis beyond approximately 100 cycles in unidirectional (UD) laminates and within 10 thermal cycles for angular-ply samples [177, 178, 179]. Cracking can be induced at earlier cycles by reducing the temperature further [180, 181, 182, 183]. Micro-cracking reduces the mechanical performance of CFRP and according to Kaw [184], tends to instigate from the interfaces of the composite (where matrix materials and fibre sizing diffuse into one another creating a weak boundary layer). It can moreover be logically inferred that hot and cold expansions and contractions, respectively, increase localised stresses between the fibre and matrix materials, thus damaging the interfaces [185, 186, 187, 188]. The idea that thermal cycling can affect the composite properties within such a short number of cycles is of importance as thermal cycling in e.g. fixed wing aircraft and wind turbine blades is regular and the integrated design of CFRP within these structures should account for the impact of thermal cycling over the expected product service-life, *alongside* the degradation of CFRP properties due to fatigue.

The fracture behaviour of quasi-isotropic CFRP laminates (UT500/135 and T800S/3900-2B) in flexural fatigue is affected by temperature in that; whereas under ambient or low temperatures fractures tend to be localised to the outermost fibres of the flexural specimen, as temperatures increase, so too does the depth at which fractures will propagate [189]. This brings to light the more adverse effects of high temperatures on the fatigue life of quasi-isotropic CFRPs as damage propagation under higher temperatures will more detrimentally affect their residual load carrying capacities. These fracture patterns are very different to the temperature induced fracture patterns of unidirectional CFRP under flexure, which at lower temperatures (60°C) are tensile fracture dominant, at mid-range temperatures (130°C) are compressive fracture dominant and at very high temperatures (260°C) exhibit microbuckling [189]. Quasi-isotropic laminates are somewhat special materials as they exhibit several fibre orientations. Fibre orientation tends to guide fracture in composites however, fibre orientation specific fractures are also affected by both cyclic loading, and temperature [190], with 45° oriented coupons showing the largest variation in failure pattern from equivalent tensile fractured samples. What is interesting is that when comparing the *S-N* curves of $[0]_8$ and $[0, 0, +45, -45]_s$ from −20°C to +100°C, it can be shown that $[0]_8$ composites have a larger overall reduction in their strength properties than $[0, 0, +45, -45]_s$, though the rate of decline in strength is greater in the $[0, 0, +45, -45]_s$ as compared to the $[0]_8$ composites [191]. Similarly, Wu found that the [0/45] orientations were

hardly affected by heat (up to the curing temperature) in terms of strength degradation, but that [0/90] would lose considerable strength under fatigue as a result of heating [192]. As such, it would make sense to use high temperature resistant CFRP in cross-ply CFRP (e.g. AS4/PEEK, G40-800/5260) [193] however, even these are ultimately subject to the properties of the matrix materials, and the orthotropy of CFRP laminates. Premature fatigue failure through matrix-cracking [194] in cross-ply CFRP at higher temperatures can nevertheless be circumvented by increasing the thickness of the plate through the addition of extra constituent plies within the plate [196].

Miyano and co-workers [197, 198] posit that the tensile fatigue life of time and temperature dependent unidirectional CFRP can be predicted if four hypotheses are applied to the predictive model. Their predictions are quite accurate for CFRP using PAN based carbon fibre/epoxy composites [197] and T300/2500, T300/PEEK and XN40/25C composites [198]. The four hypotheses upon which their model is based include:

1. That failure at a constant strain rate, in creep and in fatigue are the same
2. That the same time-temperature superposition principle is used for all failure strengths
3. That the model uses a linear cumulative damage law for monotonic loading
4. That there is a linear dependence of fatigue strength on the stress ratio.

3.2. Effects of water on CFRP and fatigue

Moisture and water enter CFRP composites through mixed modes of Fickian-diffusion [199, 200, 201], filling of voids within the matrix bulk [202], and wicking at the fibre-matrix interfaces [203]. The volume of water that will enter CFRP will therefore depend highly on the type of matrix polymer that is used. Epoxy matrix CFRPs tend to gain more weight through moisture absorption than vinyl ester and urethane acrylate based CFRPs [204] since epoxides have molecular structures with larger numbers of hydrogen bonding potential per unit volume than esters and acrylates. Similarly to heat-induced swelling, CFRP will swell when water enters its structure and the extent of swelling will determine the level of damage caused to the interfaces through both shear [205] and compressive movement [206]. The logical consequence of water ingress, swelling and the internal localisation of stress, is that the mechanical properties of CFRP are detrimentally affected [174]. The affect of water absorption into CFRP has been summarised with respect to damage mechanisms by Selzer and Friedrich [207]. In their paper, they find that all forms of damage occur in water saturated CFRP at lower stress levels than for dry materials. Cracking in 90° layers will occur prior to cracks in 45° layers, which are precursors to delamination. Importantly, the ratio of catastrophically failed CFRP to damage free CFRP is ca. 4.5:1 in fully water saturated composite, while it is only 3.2:1 in dry CFRP, indicating that fatigue damage tolerance is approximately one-third less in wet CFRP as compared with dry CFRP. There are nevertheless, distinct differences between Mode I and Mode II cracking of CFRP in water and dry conditions. [208]. Mode II cracks tends to dominate with respect to water absorption time, while Mode I cracking is guided by the number of loading cycles imposed on the material. The Mode II maximum energy release rate of water conditioned end notched epoxy matrix CFRP (T800/3900-2) flexure specimens in fatigue tends to be lower than equivalent dry samples [208] and this presumably relates to the plasticisation of matrix material by water absorption [208, 208]. Komai et al. [210] further hypothesise (using T-1/347 and MM-1/982X ±45 CFRP laminates) that the water induced swelling of matrix material increases the concentration of stress at fibre-matrix interfaces and between individual laminates. This in turn causes microcracking at the fibre-matrix and interlaminar interfaces, as well as interfacial debonding [211], which promotes further water absorption and results in a rapid degradation of the fatigue life of water-immersed CFRP as compared to dry CFRP. This said nevertheless, the dimensions of larger scale fractures in cyclically loaded CFRP are an inverse function of water content. Chiou and Bradley [212] using $[+45/0/-45/90]_s$ epoxy matrix CFRP (IM7/TACTIX556) find that the crack area does in fact decrease with the CFRP moisture content. This highlights a clear difference in understanding the role of fracture and their locations within CFRP. It could be postulated based on these reports, that microcracks in the early stages of fatigue are confined to the interfaces. As they build up they encourage greater water absorption and thus, plasticisation of the matrix. At the later stages in the fatigue life (cf. Figure 10) larger scale fractures dominate failure and the crack areas of highly plasticised CFRP are reduced as there is more plastic deformation of the matrix, and thus reduced matrix cracking (as compared with dry CFRP). The properties of the matrix materials in CFRP are also a guide to the mechanisms of failure [213] since polymers absorb water at different rates, swell to different extents, and are also mechanically affected by water to different levels. PEEK for example is a semi-crystalline thermoplastic polymer with excellent properties of toughness. The hygrothermal conditioning of PEEK matrix CFRP is reported to have little influence on its T-T fatigue life compared to dry composites [214]. This is in stark contrast to epoxy matrix CFRP, which shows not only a strong decline in properties compared to dry composites, but are moreover highly sensitive to the loading regimen (R ratio) [215, 216, 217, 218].

4. Fatigue damage in CFRP composites

Composite fatigue damage mechanisms are complicated because composite materials are intrinsically inhomogeneous. Fatigue can be characterised by the initiation and growth of damage. This includes different competing

modes of damage, as well as the complex interactions that occur between them [219, 220, 221, 222]. Different stages of damage can be described by the Paris law [223]. In this law, the crack growth rate correlates to the applied energy release rate of the composite. However, damage initiation is still somewhat of a conundrum and has been only sparsley touched upon in the literature. A simple expression reported by Corten et al. describes the phase of damage initiation as the time required for a crack to form and reach a detectable size [224]. Figure 17 shows the evolution of cyclic damage in composites, as has been reported in literature [224, 225, 226]. Three distinct stages are shown in Figure 17. In the 1st stage intralaminar cracking occurs, where cracks along the fibre-matrix interfaces or within the matrix can propagate parallel to the fibre orientation. The 2nd stage is characterised by interlaminar shear stresses, resulting in crack growth between the fibre-plies (delamination). In the 3rd stage, fibre breakage occurs transverse to the orientation of fibres, resulting in fibre or fibre ply breakage [224, 225, 226]. A schematic representation of the aforementioned three modes of damage in FRP is provided in Figure 18. Understanding and standardising test methods related to delamination and fracture toughness has been a focus point in numerous research articles [227, 228, 229, 230]. Generally in composites, fatigue damage can take the form of any or all of the following; matrix cracking and fibre-matrix interfacial debonding in the off-axis layers, delamination, fibre fracture, matrix failure, fibre micro-buckling and void growth. These forms of damage may interact with one another to transform damage from one form to another. Figure 19 illustrates damage evolution during the fatigue life of a composite laminate with 0° plies and off (loading) axis plies [219].

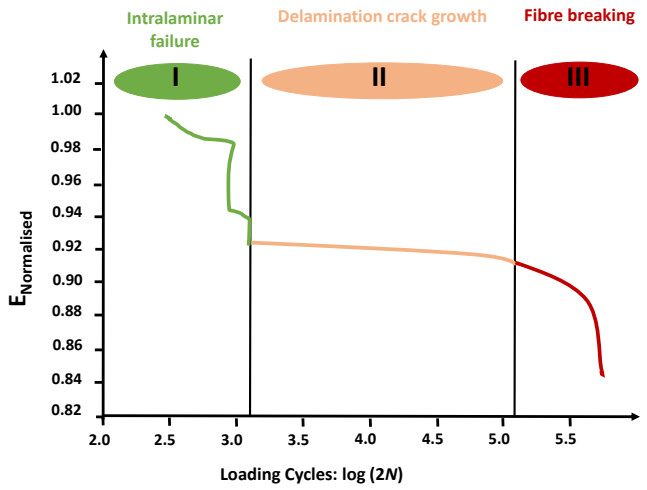

Figure 17. Fatigue damage evolution in composites. Inspired by the work of [225].

Structural components made of CFRP are often subjected to complex fatigue load histories. To simplify the analysis of fatigue damage, researchers usually use con-

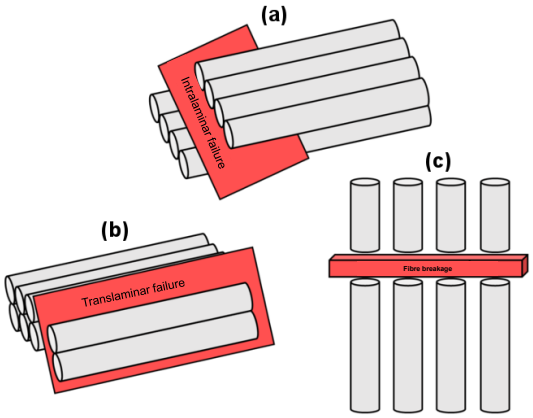

Figure 18. Representative delamination modes in FRPs: (a) intralaminar failure between the fibre layers (b) delamination and (c) fibre breakage.

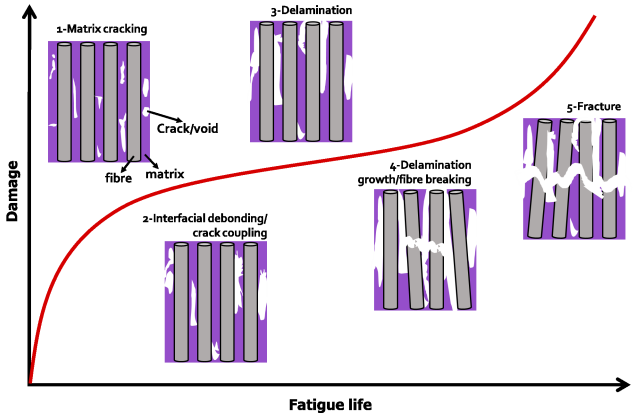

Figure 19. Damage modes and the characteristic damage state (CDS) during the fatigue life of composite laminates. Inspired by the work of [219].

stant stress ratios, R, frequencies and comparable waveforms. The fatigue life of CFRP composites is highly dependent on the stress ratio [17, 231, 232, 233, 234, 235, 236, 237, 238, 239, 240, 241, 242, 243, 244, 245] and this influences the shape of the $S-N$ curve, which typically follows the form $S = \sigma_{TU}(mlogN + b)$, where S is the maximum fatigue stress, N is the number of cycles to failure, σ_{TU} is the average static strength, and m and b are constants where m describes the slope and b is the stress intercept of the $S-N$ curve. It is worth noting that low values of m and high values of b indicate a high fatigue strength. Unlike the fatigue analysis of metallic materials where a linear Goodman [246] diagram has broadly been used to identify fatigue limits, for CFRP laminates, the fatigue limit cannot be determined using a simple linear approach. An effective method of evaluating S-N curves for CFRP with constant amplitude fa-

tigue loading at different R values is through a constant fatigue life (CFL) diagram, Figure 20, [244, 245]. CFL diagrams describe the fatigue behaviour of CFRP plotting the alternating stress amplitude against the mean stress. These diagrams become asymmetric due through differences in the tensile and compressive strengths. The alternating stress amplitude form the fatigue loading of CFRP laminates tends to take a maximum value at a nonzero mean stress [241, 242, 247, 243]. For this reason, many systematic studies that have been carried out to identify the most suitable method to recognise a CFL diagram for CFRP laminates in fatigue. Many posit that these are bell-shaped curves, regardless of the types of carbon fibres and matrix resins used [239, 241, 242, 247, 243]. The CFL diagram for has been used for several different kinds of CFRP laminates [248, 249, 250, 251, 252, 253, 254]. Recently, it was shown by Kawai(2016)[255] that a unidirectional carbon/epoxy composite, under (T-T) loading ($0 < R < 1$) and (T-C) ($R < 0$) loading, has a steeper S-N curve slope than (C-C) loaded ($R > 1$) composites. This observation is consistent with the quasi–static behaviour of the composites, which are stronger in tension than in compression. Additionally, Vassilopoulos et al. [256] showed that the S-N curve at $R = 0.1$ was steeper than that at $R = 10$ due to that the accumulation of matrix cracks under tensile fatigue loads was more pronounced and more catastrophic. However, for specimens cut in the transverse direction (90°), the most critical loading mode seems to be in (T-T) at $R = 0.1$, compared to those of $R = -1$ and $R = 10$, as reported by Vassilopoulos et al. [256]. Here, the absence of fibres along the loading direction made the material more vulnerable to (T-T) loading. In addition, the authors showed that for on-axis composites that failed due to fibre breakage, the reversed loadings ($R = -1$) was more detrimental to the fatigue life than the tensile loadings ($R = 0.1$).

The degree of fatigue damage in CFRP relates to the properties of the fibres and matrices. Relevant properties include fibre size, stiffness, strength, orientation and stacking, and the viscoelastic properties of the matrix polymer. Composites containing stiff fibres such as carbon are often considered as being more resistant to fatigue that lower stiffness fibres. This is because they are more adept at carrying load and as such, the weaker component of composites (the polymer matrix), will extend less as a function of loading when the fibres are stiff, thereby reducing matrix damage. The loading modes are important as they govern the dominant damage mechanisms in fatigue, the most damaging loading mode being acknowledged as tension-compression (T-C). Fibre failure criteria under such modes can be either tensile or compressive [30, 257, 258], with compressive failures often instigated by cross-shear within the fibres, or buckling rupture of the fibres [261, 262, 263, 264]. Tensile fibre failures contrarily [259, 260] can be associated to fibre pull-outs by debonding, and fibre cross-fractures. This said, fibre pull-outs by debonding are in fact, a function of the bond shear strength between the fibre and matrix. Compressive failure is sometimes considered a design limitation in UD CFRP, since compressive strengths of UD CFRP are often less than 60% of their tensile strengths. Matrix failure in fatigue may occur either within a ply, or between plies (delamination). Matrix failure may also occur at the fibre/matrix interface, which in turn leads fracture propagation away from the interface and into the matrix bulk. CFRP delamination occurs due interlaminar stresses generated between the plies, and is often a result of cracks/voids in the matrix phase [265, 229]. Gamstedt et al. [18] researched the influence of matrix type on fatigue life in UD CFRPs using both thermoplastic (polyetheretherketone, PEEK) and thermosetting matrices (epoxy toughened with a thermoplastic additive). The two composite cases were loaded in tension-tension along the fibre direction and fatigue tests revealed that the thermoset matrix CFRP had a higher resistance to fatigue failure than the thermoplastic matrix CFRP, the fatigue life being most likely guided by matrix cracking [266, 267, 268]. Petermann et al. [232] studied the fatigue life of carbon-epoxy laminates with ±45° angle-ply orientation under tension-tension at high stress ratios (between 0.40 and 0.86 times of the static tensile strength). They reported that fatigue damage was governed by cyclic creep due to the absence of 0°-layers angle-ply laminates [232]. It is well-established that the stress ratio affects delamination and delamination growth [229, 269, 270, 271, 272]. Other causes of delamination may arise through machining and/or the cutting of FRP laminates, residual stresses from the manufacturing process (e.g. curing), or material irregularities and geometrical characteristics including edge effects, holes and ply-drop offs [20].

Delamination is a failure mode possibly requiring the least amount of energy. It is hence a major source of concern for composite designers [273]. The fact that this is difficult to detect during service makes this a more pronounced problem still [274], as it reduces the load carrying capacity of the composite and may lead to premature failure. Delaminations can be triggered by fatigue loads as it is almost impossible at present, to manufacture a composite without defects generated either during the curing process or during machining [275]. Fatigue delamination in composite structures is more complex than for metals where cracks deviate to grow predominantly in the mode I loading direction. Indeed, crack growth is usually constrained at the interface between plies and therefore the delamination mode occurring during the service life will most likely be a mix of modes I, II and III. In fact, the study of delamination in the fatigue of fibre reinforced composites has been the subject of several recent review papers [276, 277]. A brief overview of this topic will be given here but the full study of fatigue delamination is beyond the scope of this review.

There exists three main ways of experimentally characterising fatigue delamination [276]. These are; crack propagation, which is the measure of the rate of crack growth

per cycle as a function of the stress intensity factor or the strain energy release rate (SERR), crack onset, which is a measure of how many cycles are required to visibly extend an existing crack, and crack initiation, which is a measure of the number of cycles required to generate a crack in an ideal (defect free) composite. The crack initiation tests have so far not been studied extensively and show large scatter in the results [278]. This, as mentioned previously, is probably caused by the presence of small defects within the composite. Crack propagation tests are usually carried out using the ASTM standard for metals for mode I [279] and allows the determination of the whole crack growth rate curve. Crack onset fatigue delamination testing in mode I for composites is the only one for which a standard exists [280]. This leads to the determination of the SERR as a function of the number of cycles required for crack growth. However, it is often assumed in the literature [276] that a small crack propagation is equivalent to fatigue crack onset and that therefore these phenomena are the same.

There are three types of delamination modes affecting the growth of a crack: mode I (normal opening), mode II (in-plane shear) and mode III (shear scissoring or out of plane shear). Modes I and II delamination, at least in the case of static loading, are quite well understood. However, mode III loading has not been studied extensively and it is usually assumed that mode III and mode II delamination have the same properties, which is conservative, considering mode III has been shown to have a higher interlaminar fracture toughness [281]. Mode II delamination toughness is usually higher than mode I toughness for composite materials [282], although it has been shown during crack propagation tests that the difference in crack growth rate between the different modes reduces [283] as the cycle count increases and eventually disappears for carbon/epoxy. It was also shown that the threshold below which no fatigue damage occurs is independent of the loading mode [284]. Therefore, the effect of mixed mode ratio on fatigue delamination for high cycle fatigue can be considered negligible.

When the maximum SERR near a crack tip is close to its interlaminar fracture toughness, the delamination propagates rapidly and the failure is similar to that observed in a quasi-static test and therefore the R ratio has no influence on the crack growth rate. However, as the maximum value of the SERR is reached as a loading cycle reduces, it has been shown that the effect of the R ratio on fatigue delamination increases [285]. The damage threshold and the exponent of the Paris law curve are lower for lower R ratios for mode I and mode II crack growth rates in carbon/epoxy composites for $R = 0.1$ and $R = 0.5$. This is also true for mixed mode delamination [286].

Other factors have an influence on the fatigue delamination of composite structures such as the loading frequency, loading sequence, environmental factors such as moisture, water uptake and temperatures as well as matrix properties such as the brittleness [276]. However, these topics are not discussed in this paper. If further information is required, the reader is directed to review papers dedicated to fatigue delamination [276, 277].

5. Fatigue modelling of CFRP

A few review papers have been written on the modelling of fatigue in FRP [297, 298, 299, 22]. While Pascoe et al. focused solely on methods predicting the fatigue delamination growth in composites [297], Degrieck and van Paepegem compared a wider variety of modelling methods for both UD and textile FRP composites [298, 299]. They proposed a classification system to separate the different modelling techniques: (i) fatigue life models based on experimental data such as S-N curves, (ii) phenomenological models which are not based on physical mechanisms but rather, on observed macroscopic properties during fatigue, such as residual strength and stiffness, and (iii) progressive damage models which take into account damage mechanisms and either, correlate them to mechanical properties (stiffness and strength), or, measure the damage growth (delamination size, cracks per unit area). The same classification system will be used in this section.

5.1. Fatigue models - a general overview

In 1973, Hashin and Rotem developed one of the first fatigue failure models for composites [30]. They considered two different failure mechanisms; fibre-failure and matrix-failure. They proposed a failure criterion for each mode of failure based on three separate S-N curves; longitudinal tensile strength, transverse tensile strength and shear strength. These curves can be obtained experimentally by off-axis tensile testing of coupons under uniaxial constant amplitude stresses. In Equations 1 and 2, σ_a represents the longitudinal fiber stress, σ_T the transverse stress, τ the shear stress and σ_a^S, σ_T^S and τ^S the ultimate tensile, transverse and shear strengths, respectively. This model is only applicable to unidirectional laminates.

$$\sigma_a = \sigma_a^S \tag{1}$$

$$(\frac{\sigma_T}{\sigma_T^S})^2 + (\frac{\tau}{\tau^S})^2 = 1 \tag{2}$$

A number of fatigue models using S-N curves and various failure criterion were developed in the subsequent years to account for multiaxial laminates which are restricted to the two failure modes mentioned above. As most of these models were developed before the early 2000s, they are not presented in detail in this paper.

Another common approach in fatigue life modelling is to use constant fatigue life (CFL) diagrams. Here, the cycles to failure are plotted as a function of mean stress on the x-axis and alternating stress on the y-axis. They are useful because they show the mean stress sensitivity of composites, as have been observed in tests. Through extensive experimentation on the strength and fatigue life of aerospace CFRP laminates, Harris et al. [300] showed that

the CFL envelopes for these materials is asymmetric and nonlinear, and that their peak positions are shifted to the right of the alternating stress axis. Ramani and Williams [301] eperimented on the fatigue behaviour of notched and un-notched carbon/epoxy composites. They found that the maximum of the CFL envelope does not occur at R=-1 but rather, at around R= −0.43 and for a positive mean stress. Based on these previous studies, Kawai et al. [302] proposed what they called an anisomorphic CFL diagram, taking into account the asymmetry of the curve as well as the occurrence of the peak envelope at a positive mean stress. It can be built using only the static strength in tension and compression and a reference S-N curve for a critical stress ratio equal to the ratio of compressive to tensile strength. It was shown to be valid for the prediction of fatigue failure in non-woven carbon/epoxy laminates [302]. The approach was extended to predict the fatigue of woven composites for different temperatures in a later study [303]. Their approach involved using the critical stress ratio defined above as the ratio between compressive and static strength $\chi = \sigma_C/\sigma_T$. The CFL is then divided into two domains, tension-tension dominated and compression-compression dominated. These two domains have smooth nonlinear curves connected by a point as shown in Fig. 20 Therefore, the envelope of the anisomorphic CFL diagram can be defined by the following piecewise function:

$$-\frac{\sigma_a - \sigma_a^{(\chi)}}{\sigma_a^{(\chi)}} = \begin{cases} \left(\frac{\sigma_m - \sigma_m^{(\chi)}}{\sigma_T - \sigma_m^{(\chi)}}\right)^{2-\psi_{(\chi)}^{k_T}} & , \quad \sigma_M^{(\chi)} \le \sigma_M \le \sigma_T \\ \left(\frac{\sigma_m - \sigma_m^{(\chi)}}{\sigma_C - \sigma_m^{(\chi)}}\right)^{2-\psi_{(\chi)}^{k_C}} & , \quad \sigma_C \le \sigma_M < \sigma_M^{(\chi)} \end{cases} \tag{3}$$

where σ_m, σ_a, σ_T and σ_C are the mean stress, stress amplitude, tensile and compressive strengths. ψ_χ is the fatigue strength ratio and takes a value in the range $\psi \in [0, 1]$, χ is the critical stress ratio and k is an exponent used to transform a straight line into a parabola in tension $(_T)$ and compression $(_C)$, and are both based on empirical data.

The reference normalised S-N curve then has the following form:

$$2N_f = \frac{1}{K_\chi}\frac{1}{(\psi_\chi)^n}\frac{\langle 1-\psi_\chi\rangle^a}{\langle \psi_\chi - \psi_{\chi^{(L)}}\rangle^b} \tag{4}$$

where the angular brackets represent the function defined as $\langle x\rangle = max\{0, x\}$, $\psi_{\chi^{(L)}}$ is the normalised fatigue limit and K_χ , a, b and n are material constants which can be determined by fitting Equation 4 to fatigue data at the critical stress ratio. This model was shown to give adequate results for woven carbon/epoxy laminates.

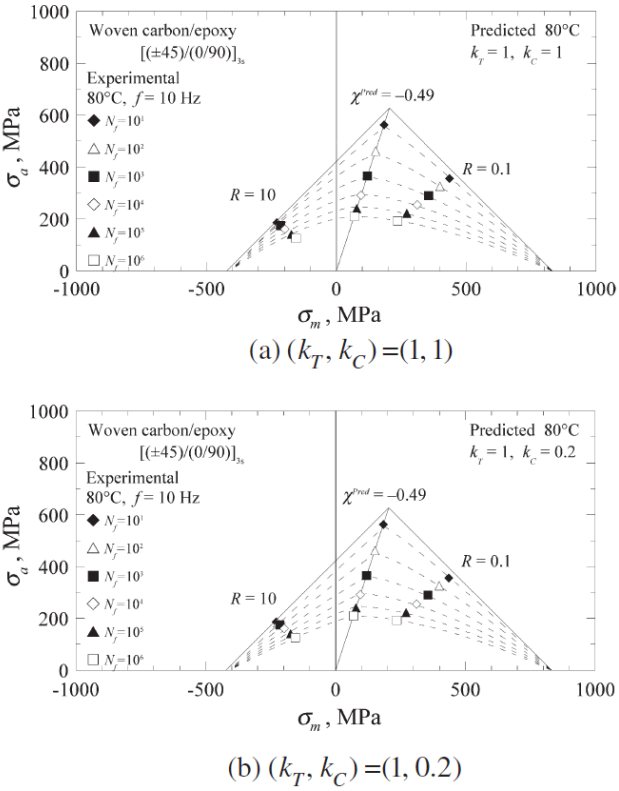

Figure 20. Example of CFL Diagram for a Temperature of 80°C. From [302], reproduced with the permission of Elsevier.

Fatigue life models were the first fatigue models developed. They are often used as they do not require any understanding of the physical damage mechanisms and are very simple to use. However, these models require a large amount of experimental data and are usually calibrated for one specific case-study. The breadth of applicability to other problems is therefore very limited.

5.2. Phenomenological models

5.2.1. Residual strength models

Based on previous work carried out on the development of a residual stiffness model [304], and assuming a linear stress strain response until failure, Whitworth [305] proposed a strain failure criterion to eliminate the failure stiffness from his model and obtain the following fatigue life relationship:

$$N = exp\left\{\frac{1}{h}\left[\left(\frac{c_1 S_U}{S}\right)^{\frac{m}{c_2}} - 1\right]\right\} - 1 \tag{5}$$

where parameters h and m depend on the applied stress, loading frequency and environmental conditions, c_1 and c_2 are constants determined experimentally, N is the number

of cycles to failure, S_U is the ultimate strength and S is the maximum applied stress.

Whitworth further proposed the following relation for strength degradation [304]:

$$S_R^\gamma = S_U^\gamma - [S_U^\gamma - S^\gamma]\frac{n}{N} \tag{6}$$

where γ is a material constant determined experimentally and S_R is the residual strength. Once all the material parameters have been determined, Equations 5 and 6 can be used to determine the residual strength. Failure occurs when the maximum applied stress equals the residual strength. Whitworth also assumed that the ultimate strength was a statistical variable that he represented with a 2 parameter Weibull distribution. The model was validated on T300/5280 graphite/epoxy laminates which were tested under constant amplitude loading for 50,000 cycles. The median residual strength after the test was 353 MPa which the author considered sufficiently close to the value of 371 MPa predicted by the model.

Yao and Himmel [306] proposed a residual strength model for FRP polymers that could capture rapid degradation in the early stages of fatigue life. The model was also able to account for level and slow degradation that occurs in the middle of the fatigue life, as well as rapid degradation in the final cycles. For tension-tension fatigue, they proposed the following relationship:

$$R(i) = R(0) - [R(0) - S]\frac{\sin(\beta x)\cos(\beta - \alpha)}{\sin(\beta)\cos(\beta x - \alpha)} \tag{7}$$

where $R(i)$ is the residual strength at the i^{th} cycle, $R(0)$ is the static strength, S is the maximum stress in the loading cycle, α and β are constants to be determined experimentally and $x = i/N_f$.

For specimens in compression-compression fatigue, the following degradation law was proposed:

$$R(i) = R(0) - [R(0) - S](\frac{i}{N_f})^\nu \tag{8}$$

where ν is a strength degradation parameter defined in their study as 0.64. By using fatigue data obtained by Harris et al. for T800/5245 laminates [307], the model was validated and showed to have good predictive capability.

Compared to other types of CFRP fatigue models, only a few models have been found that model the pure residual strength of CFRP. The main drawback of these models is that, they are unable to account for the stiffness degradation (observed experimentally), though they are still able to predict the fatigue life. The primary issue of contention is thence that these models are not able to predict the deformation of composites throughout their fatigue life.

5.2.2. Residual stiffness models

Residual stiffness is not simple to model as there are several overlapping factors including the rheological responses, bulk molecular kinematics and variations in molecular orientations at fibre interfaces, each as a function of loading time and frequency [308, 309, 310, 311]. Yang et al. [312] developed a stiffness reduction model assuming the stress-strain curve to failure as linear. Their model is valid for laminates with fibre-dominated properties. However, in the case of laminates with matrix-dominated properties, the assumption of linearity between stress and strain to failure is incorrect. They proposed the following degradation law:

$$\frac{dE(n)}{dn} = -E(0)Q\nu n^{\nu-1} \tag{9}$$

where $E(0)$ is the static stiffness, Q and ν are parameters dependent on the applied stress level, stress ratio and loading frequency. Yang et al. defined $E(0)$ using a log-normal statistical distribution in their model. The model assumed that failure occurred when the strain in the specimen was equal to the static ultimate strain. The model was validated using graphite/epoxy coupons in tension-tension fatigue. The predicted and experimental fatigue life curves were noted to correlate well with one another.

Khan et al. [313] proposed a stiffness reduction model where they created a damage variable, D, that related to stiffness in the following way:

$$\frac{E}{E_0} = 1 - cD \tag{10}$$

$$c = \pi(2\frac{E_A^2}{E_T})^{1/2}\left[\frac{1}{(E_A E_T)^{1/2}} + \frac{1}{2G_A} - \frac{\nu_A}{E_A}\right]^{1/2} \tag{11}$$

where E_A, G_A, ν_A are the Young's modulus, shear modulus and Poisson's ratio in the axial direction, respectively, while E_T is the transverse modulus of the undamaged specimen. It is therefore possible to relate the damage growth per cycle to experimentally measured reductions in stiffness. Failure is assumed to occur when the maximum strain in a cycle is equal to the static ultimate strain. The value of the damage variable at failure can also be calculated. The cycle count to failure can be obtained by integrating the damage variable from its initial to its final value:

$$N_f = \int_{D_i}^{D_f} \frac{dD}{f(\Delta\sigma, D)} \tag{12}$$

5.3. Progressive damage models

Shokrieh and Lessard [314] proposed a progressive fatigue damage model combining stress analyses, failure analyses and material degradation. The modelling method used is explained in the form of a flowchart in Figure 21. A finite element stress analysis is first carried out on a specimen, using solid elements. Edge effects are accounted for by using a higher element density near edges and other areas of stress concentration such as holes and notches. Iterative schemes are used to account for nonlinearity in

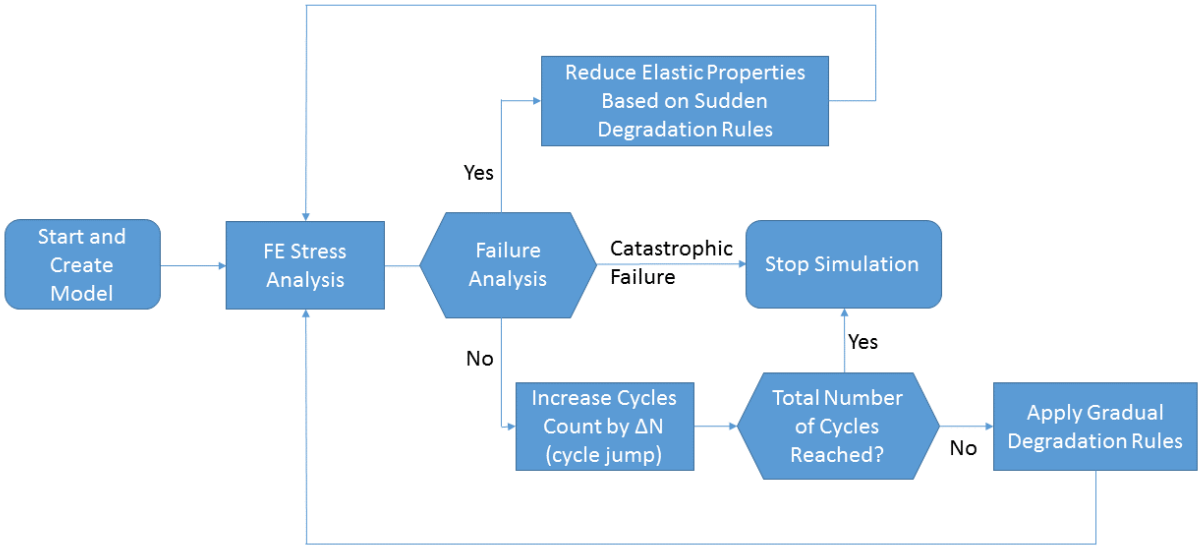

Figure 21. Flowchart of Shrokrieh and Lessard Progressive Damage Model. Figure inspired by the work of [314].

the stress state when failure occurs. A failure analysis is carried out considering seven different failure modes; fibre tension and compression, matrix tension and compression, normal tension and compression, and fibre-matrix shearing. The failure criteria used are similar to the Hashin static failure [257] criteria but the material properties are functions of cycles, stress state and stress ratio. Additional parameters have been added to account for material nonlinearity. The fibre tension fatigue criterion for $\sigma_{xx} > 0$ is:

$$g_{F+}^2 = \left(\frac{\sigma_{xx}}{X_T(n,\sigma,\kappa)}\right)^2 + \left(\frac{\frac{\sigma_{xy}^2}{2E_{xy}(n,\sigma,\kappa)} + \frac{3}{4}\delta\sigma_{xy}^4}{\frac{S_{xy}^2}{2E_{xy}(n,\sigma,\kappa)} + \frac{3}{4}\delta S_{xy}^4(n,\sigma,\kappa)}\right) + \left(\frac{\frac{\sigma_{xz}^2}{2E_{xz}(n,\sigma,\kappa)} + \frac{3}{4}\delta\sigma_{xy}^4}{\frac{S_{xz}^2}{2E_{xz}(n,\sigma,\kappa)} + \frac{3}{4}\delta S_{xz}^4(n,\sigma,\kappa)}\right) \tag{13}$$

and failure occurs if $g_{F+} > 1$. Here, X_T, S_{xy}, S_{xz} are the residual longitudinal tensile strength, the in-plane and out-of-plane residual shear strengths, respectively. E_{xy} and E_{xz} are the residual in-plane and out-of-plane shear stiffness values, repsectively. σ_{xx}, σ_{xy} and σ_{yz} are the longitudinal, in-plane shear and out-of-plane shear stresses in the elements, respectively. δ is a material nonlinearity parameter which is considered to be constant. For the failure criteria of the other failure modes refer to [314]. The final part of the fatigue model considers the material degradation, which is separated into two parts; sudden and gradual degradation. Each failure mode is associated with some of the material properties being reduced to zero. For matrix compression failure for example, E_{yy}, ν_{yz} and νyz are reduced to zero. Fibre tension and compression are considered to be catastrophic failure modes and therefore are followed by a reduction of all material stiffness values and Poisson's ratios to zero. The authors also developed a generalised residual material property degradation as:

$$R(n,\sigma,\kappa) = \left[1 - \left(\frac{\log(n) - \log(0.25)}{\log(N_f) - \log(0.25)}\right)^{\beta}\right]^{1/\alpha} \cdot (R_S - \sigma) + \sigma \tag{14}$$

$$E(n,\sigma,\kappa) = \left[1 - \left(\frac{\log(n) - \log(0.25)}{\log(N_f) - \log(0.25)}\right)^{\lambda}\right]^{1/\gamma} \cdot (E_S - \frac{\sigma}{\varepsilon_f}) + \frac{\sigma}{\varepsilon_f} \tag{15}$$

where $R(n,\sigma,\kappa)$ and $E(n,\sigma,\kappa)$ are the residual strength and stiffness, N_f is the fatigue life, σ is the maximum applied stress, R_S and E_S are the static strength and stiffness, α, β, λ and γ are curve fitting parameters and ε_f is

the average strain to failure. Shokrieh and Lessard compared their model predictions to experimental data on pin and bolt-loaded graphite/epoxy laminates. These specimen were chosen for their complexity and because of the presence of stress concentrators. A good agreement was found to exist between the predicted and measured fatigue life. The main disadvantage with this model was that it required considerable experimentation for each application to obtain the gradual degradation parameters.

A similar model was developed by Papanikos et al. [316] combining stress, failure analyses and material degradation. Seven failure modes were considered but simpler formulations were used with no nonlinear parameter. For delamination in tension and compression, the Ye delamination criterion was used [320, 321], while 3D static Hashin Criterion [257] was used to predict matrix tensile and compressive failure as well as fibre-matrix shearing. In previous work [322], the authors compared the predicted elastic responses and failure loads of a bolted joint in a graphite/epoxy composite to experimental results. They found that better predictions were obtained using the Maximum Stress Criterion (MSC) for fibre failures in tension and compression than the 3D Hashin Criterion. They also used a set of rules for sudden degradation that yielded a closer fit to their experimental data. Therefore, unlike the model by Shokrieh and Lessard, once failure occurs, the associated stiffnesses are not reduced to zero. Also, the generalised residual property degradation rules used were simplified, using a linear stiffness reduction and a second-order polynomial for strength reduction: $E(n) = [A(n/N_f) + 1)]\, E_S$ and $R(n) = \left[B(n/N_f)^2 + C(n/N_f) + 1\right] R_S$; where $E(n)$ and $R(n)$ are the residual stiffness and strength, E_S and R_S are the static stiffness and strength, A, B and C are material parameters obtained experimentally. Only the maximum and minimum cycle loads were modelled to account for the stress ratio effects. As in some cases, millions of cycles can occur before failure, conducting a full stress analysis at each cycle would require tremendous amounts of CPU time. Therefore, the authors proposed applying a cycle jump between each FE stress analysis, during which only material property degradations were applied. However, the authors did not provide any recommendations on what increment to use for the cycle jump or how that affects the accuracy of the model. The model was validated with CFRP laminates tested in tension-compression. It was shown to not only give an accurate prediction of the fatigue life but also predicted the onset and growth of the correct damage modes. Indeed, both the model and experimental results considered delamination as the main failure mode for low stresses and fibre tensile failure for high stresses.

Using a similar approach, Kennedy et al. [317] developed a model by modifying the Puck Failure criterion [318] to analyse fatigue in FRPs. They carried out a stress analysis at the ply level, followed by a failure analysis. A separate analysis was carried out on the fibre responses and

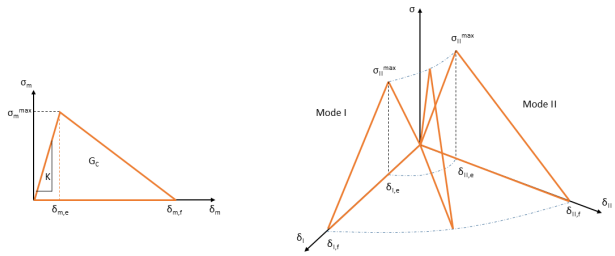

Figure 22. Bilinear constitutive law for cohesive elements (a) and its definition for mixed-mode loading (b). Figure inspired by the work of [327].

the matrix responses to shear and normal stresses in the FRP primary axis. The fibre direction strength was reduced according to a linear degradation rule, while the stiffness was reduced linearly as a function of the accumulated damage. Irrecoverable cyclic strains were also calculated as a function of the degraded fibre direction modulus. Failure was considered to have occurred when the fibre direction stresses were equal to the fibre direction residual strengths. For the matrix response, a failure analysis was first carried out for Inter Fibre Failure (IFF) using modified Puck stress exposure equations [319] where the static strengths were replaced by the fatigue strengths. Here, IFF occurs when the stress exposure was greater than 1. At each cycle, the fatigue strengths used in the failure initiation criteria were reduced according to a linear degradation rule. Three modes of matrix failure were considered depending on the combination of shear and normal stresses, with Mode A corresponding to tensile normal stress and mode B and C to compressive normal stress. Before the occurrence of IFF, the shear modulus was reduced slowly for Mode A while the transverse modulus was reduced gradually for modes B and C. After IFF, both the shear and transverse moduli are reduced rapidly for Modes A and B, while mode C was taken as leading into an immediate catastrophic failure at that point. This approach required the use of material parameters that shaped the moduli degradation rules, and which were obtained experimentally. The model was validated for quasi-isotropic E-glass/epoxy samples and shown to have a good correlation with experimentally measured fatigue life and fatigue modulus degradation. However, at higher stress levels, the model did show a tendency of over predicting the modulus degradation. Although this model thus far not been used for CFRP, the authors claim that it can be applied to any fibre reinforced composite. It would nevertheless require an experimental set up for CFRP in order to obtain all the material parameters for the degradation rules.

Delamination is the failure mode requiring the least energy. Harper and Hallett [321] developed a fatigue degradation law using cohesive interface elements. These ele-

ments do not have a single stiffness but are governed by a bi-linear constitutive law shown in Figure 22, which means the displacements are initially elastic until the maximum strength is reached. Damage is then tracked by a variable and used to reduce the element stiffness. In elements which exceed their linear-elastic range, a crack tip is formed and damage initiates. The cohesive zone consists of all the damaged elements ahead of the crack tip. A static damage variable was introduced by Harper and Hallet to account for irreversible damage: $d_s = \frac{\delta_m - \delta_{m,e}}{\delta_{m,f} - \delta_{m,e}}$, where $\delta_{m,e}$ is the element displacement at the maximum stress level, $\delta_{m,f}$ is the displacement at failure and δ_m is the current element displacement. The element fails when d_s reaches 1. Cracks are assumed to propagate according to the model developed by Blanco [323]: $\frac{\partial a}{\partial N} = C\Delta G^m$, where a is the crack length, ΔG is the change in the strain energy release rate (SERR) and C and m are defined in [323], and are obtained through fatigue experimentation under modes I and II loading. Interface elements in the cohesive zone first go through quasi-static damage only, subsequently, as they get closer to the crack tip, they experience fatigue damage. A fatigue damage parameter was therefore introduced: $\frac{\partial d_f}{\partial N} = \frac{1-d_S-d_{f,u}}{L_{fat}} \frac{\partial a}{\partial N}$, where $d_{f,u}$ is the unwanted fatigue damage defined as the fatigue damage accumulated in the cohesive zone undergoing quasi-static damage, d_s is the static damage variable and L_{fat} is the length of the cohesive zone undergoing mostly fatigue damage defined in this paper as half the total cohesive zone length. Failure in an element occurs when the total damage defined as the sum of static and fatigue damage is equal to 1. The model proposed here requires the presence of initial cracks or high initial stress concentrations. May and Hallett extended the model to include a damage initiation criterion based on the material S-N curve [324]. Allegri et al. [325] adapted this model to the prediction of mode II fatigue delamination growth of moderately tough carbon/epoxy specimen. In later work, May and Hallett [221] introduced the concept of an initiation zone which is defined as the zone where elements have the highest SERR and where a crack forms. This allows for the identification of the location of a crack, and offers a new method by which means initiation and propagation can be simultaneously modelled. Allegri et al. [326] extended the model further, to account for the effect of the stress-ratio as well as mode-mixity on delamination propagation. The model has the option to include propagation thresholds. Only three independent material parameters are needed for the model, since the crack propagation threshold is neglected.

All the models proposed in [321, 324, 325, 221, 326] require that the cohesive zone length be predetermined. Kawashita and Hallett implemented a cohesive zone model using the commercial explicit FE solver LS-Dyna [327]. The SERR is calculated for each element at each time step which allows for the identification of delamination fronts (as elements with the highest SERR). Using this method, multiple delamination fronts can be modelled simultaneously. Fatigue damage accrues in the elements until failure occurs, after which the nearest neighbouring elements become part of the delamination front. As such, the cohesive zone length no longer needed to be pre-determined, but rather, only the effective element length, which is itself defined based on the damage state of the neighbouring elements. This method also allows for the tracking the damage propagation. This model was validated using carbon/epoxy central cut-ply specimens, and by using the NAFEMS benchmark for circular delamination made from carbon/epoxy. The authors claimed that a good correlation with experimental data could be obtained using a coarse grid, hence reducing computational time.

Tao et al. [328] proposed a similar model for fatigue delamination growth but a virtual fatigue damage parameter is introduced to identify crack tip fronts using local information only and without degrading elements. This ensures SERR is kept constant during identification and propagation stages. A correction factor is introduced to reduce the mesh sensitivity in the model. Delamination growth as calculated by this model was shown to have good correlation with experimental data for carbon/epoxy double cantilever beam and end notch flexure specimens.

Talreja proposed a physical based model, Synergistic Damage Mechanics (SDM) [329], combining micro-damage mechanics with continuum damage mechanics (CDM) as developed in previous works [330, 331]. The CDM approach consists of a two-step homogenisation. First the *stationary (undamaged) microstructure* containing the fibres and matrix is homogenised into a material with generally anisotropic properties. Following this, the *evolving microstructure* containing the damage is homogenised as shown in Figure 23. This process is carried out over a representative volume element which needs to carry a sufficient number of discrete entities to represent the effect of the homogenised response at point P. The damage entity tensor is then defined as the dyadic product of two vectors on the surface of a defect, a and n representing the influence of the point on the surrounding medium and unit normal to the surface: $d_{ij} = \int_S a_i n_j dS$. The average of the damage entity tensor over the RVE volume is defined as the damage mode tensor: $D_{ij} = \frac{1}{V} \sum_{k_\alpha} (d_{ij}^{(\alpha)})_{k_\alpha}$, where α is the damage mode, V is the volume of the RVE and k_α is the number of damage entities. A relationship proposed to relate stiffness reduction to the damage entity tensor, required the definition of eight material constants as well as a constraint parameter, which is a measure of the influence of damage on the response of the material and is linked to the crack opening displacement. The eight material parameters include the modulus in longitudinal and transverse direction, the shear modulus, the principal Poisson's ratio and four phenomenological damage parameters which are used to estimate the reduction in stiffness and can be calculated using the initial elastic properties and their values at a given crack spacing. A 3D FE analysis was carried out at the microscale to estimate the crack

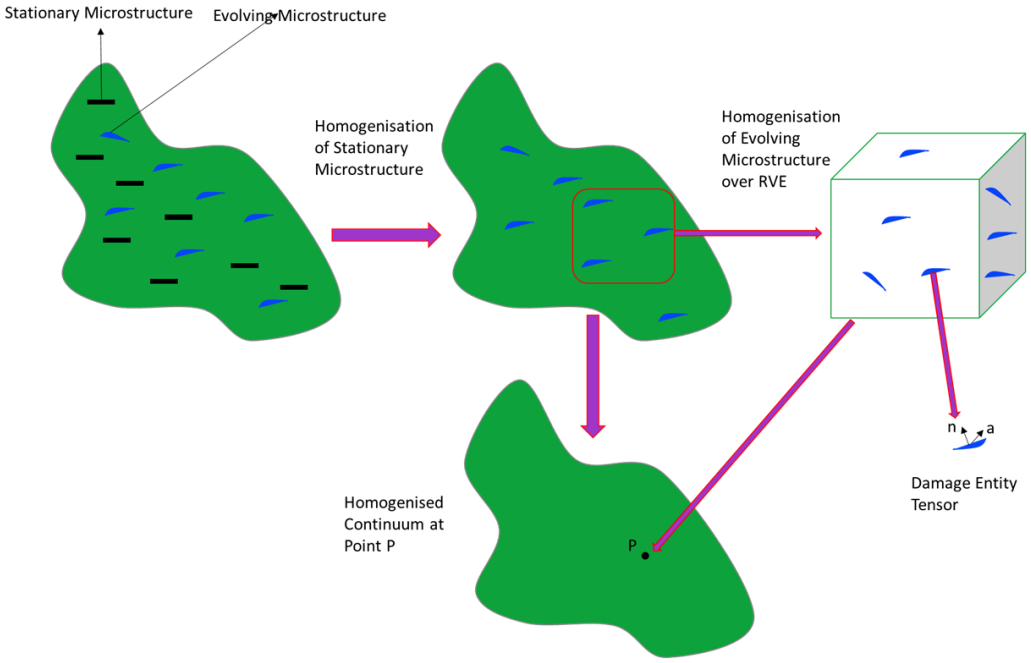

Figure 23. Description of CDM approach. Figure inspired by the work of [332].

opening displacement, and therefore the constraint parameter, κ, [333]. The material constants are determined experimentally or computationally on a reference laminate. Subsequently, the stiffness reduction is computed on the laminate scale (meso-scale). The laminate response to external loading using the reduced stiffness can be calculated (macro-scale).

In later work, Singh and Talreja extended their model to predict the evolution of crack density under a quasi-static load [334]. Singh then improved upon previous models for damage evolution by accounting for the stochastic nature of crack propagation [335]. The model was validated using a variety of carbon/epoxy cross-ply laminates. Although this approach has thus far been mostly used for quasi-static loading, it gives a framework for estimating the reduction in stiffness based on the crack opening displacement and experimentally obtained material properties. Therefore, provided the damage parameters can be obtained experimentally and the crack opening and crack sliding displacements can be obtained either experimentally or through a micro-scale FE, the evolution of crack density and stiffness during cyclic loading can be estimated. Haojie et al. [336] used non-destructive testing to obtain the transverse crack density of $[0/\pm45^\circ]_S$ laminate during a fatigue test. This allowed them to experimentally obtain the damage parameters. Therefore, using an SDM approach, they were able to predict the reduction in stiffness as a function of applied load cycles. The obtained reduction in stiffness was within 5% of the experimental results but the model was not conservative. This was because due to the limitations of non-destructive testing, only transverse cracks in the $/\pm45^\circ$ plies were considered and therefore delamination at the crack tips was ignored.

6. Conclusions

Considerable research has been undertaken to better understand the behaviour of CFRP in fatigue. Many important contributions in the area of CFRP fatigue have been described in this review, though the review is by no means exhaustive. We have focused on topic areas in CFRP fatigue of current and generic importance, which has allowed us to identify the current gaps in knowledge and understanding within this area. We will briefly describe each of the main gaps in understanding in this final conclusions section.

Much of the research presented here, has dealt with CFRP fatigue from a macro-scale view point, using primarily a mechanical and materials engineering approach to interpreting the effects of fatigue on CFRP. This is also evident from the section on modelling, where modelling methodologies have been implemented from using macro-scale physics using finite element methods. With the recent high-level developments in computational power, it is surprising that molecular modelling approaches have not been used to understand the intricate materials behaviour of CFRP in fatigue at the atomic to nano scales. Molecular modelling dynamics could be used to not only better understand the finer-scale mechanisms that essentially control the behaviour of CFRP in fatigue, but also to redesign CFRP materials structures and interfaces based on developed fine-scale understandings. Specific examples of areas

of critical importance to better understand and redesign at the low-scales include; how unloading and reloading affect the shapes/structures (and thus mechanical properties) of molecules in the matrix bulk and at fibre-matrix interfaces, the affects of water on intermolecular interactions (and energies) within the matrix bulk and at fibre-matrix interfaces, and how local heat developed through intermolecular friction affects the molecular mobility and mechanical performance of CFRPs in fatigue.

It is vital that greater research efforts are expended into understanding how strain is distributed at fibre-matrix interfaces during fatigue. There is currently a gap in our understanding on how strain fields actually evolve over a fatigue cycle at the micro and meso scales. This area is more easily tackled numerically, as it is difficult to map this reliably in fatigue given the current technologies available to us.

As has been noted in the review, fatigue testing results tend to show considerable scatter. The lack of repeatability of CFRP in fatigue is a critical concern as it depreciates engineering confidence in the material. Though we have suggested possible reasons for why significant scatter is a typical characteristic of CFRP in fatigue, there is actually very little research that has been conducted to support our hypotheses. This represents a major gap in our current understanding of CFRP fatigue and should be critically addressed so that remediation of the problems leading to scatter becomes a possibility. More focused research should therefore be conducted to deduce how manufacturing, inherent material defects, cross-link density (curing) and material homogeneity will affect the extent of scatter in CFRP under cyclic loads.

Research on the cyclic loading of CFRP has almost entirely been based on the systematic sinusoidal loading of coupons, often using simple loading modes. Yet, real structures are subjected to far more complex loading conditions and it could be argued that a worthwhile exercise would be to collate application specific real-life random spectral loading data, which can then be extrapolated to a lab-testing regimen. To include more realistic multi-directional loading conditions within such a regimen would increase the complexity of the output, perhaps even increase the extent of scatter, but it might yield enhanced insight into the actual mechanical profile of CFRP under fatigue and might positively benefit its utility in engineering structures (e.g. through improvements in safety factors and design).

7. Acknowledgments

The authors would like to acknowledge the European Union for funding this research through the following projects: MARINCOMP, Novel Composite Materials and Processes for Marine Renewable Energy, Funded under: FP7-People, Industry Academia Partnerships and Pathways (IAPP), Project reference: 612531. POWDERBLADE, Commercialisation of Advanced Composite Material Technology: Carbon-Glass Hybrid in Powder Epoxy for Large Wind Turbine Blades, Funded under: Horizon 2020, Fast Track to Innovation Pilot, Project reference: 730747.

References

[1] Ashby MF (2011) Materials selection in mechanical design, 4th Ed., *Elsevier (Butterworth-Heinemann Imprints)*, Oxford, UK
[2] Coffin Jr LF. A study of the effects of cyclic thermal stresses on a ductile metal. Trans ASME 1954;76:931–50
[3] Manson SS. Behavior of materials under conditions of thermal stress. Natl Advis Comm Aeronaut NACA TN-2933 1954
[4] Kawai M, Itoh N (2014). A failure-mode based anisomorphic constant life diagram for a unidirectional carbon/epoxy laminate under off-axis fatigue loading at room temperature. Journal of Composite Materials, 48: 571–592
[5] Hertzberg RW (1996) Deformation and fracture mechanics of engineering materials. Fourth Ed. New York, Chichester: John Wiley and Sons
[6] Boller KH (1964) Fatigue characteristics of RP laminates subjected to axial loading. Mod Plast, 41:145–50
[7] Dowling N, Siva Prasad K, Narayanasamy R (2013) Mechanical behavior of materials engineering methods for deformation, fracture, and fatigue (4th edition, International Ed. contributions by Katakam Siva Prasad, R. Narayanasamy. Boston, Mass.; London: Pearson
[8] Lemaitre J, Sermage JP, Desmorat R. (1999). A two scale damage concept applied to fatigue. International Journal of Fracture, 97: 67–81
[9] Basquin OH. The Exponential Law of Endurance Tests. Am Soc Test Mater Proc 1910;10:625–30
[10] Azeez AA, Rhee KY, Park SJ, Hui D. Epoxy clay nanocomposites – processing, properties and applications: A review. Compos Part B Eng 2013;45:308–20
[11] Altenbach H. Book Review: P. K. Mallick, Fiber-Reinforced Composites. Materials, Manufacturing, and Design. ZAMM 2009;89:921–921
[12] Paiva MC, Nardin M, Bernardo CA, Schultz J. Influence of thermal history on the results of fragmentation tests on high-modulus carbon-fibre/polycarbonate model composites. Compos Sci Technol 1997;57:839–43
[13] Davies P, Germain G, Gaurier B, Boisseau A, Perreux D. Evaluation of the durability of composite tidal turbine blades. Philos Trans R Soc London A Math Phys Eng Sci 2013;371
[14] Bathias C. An engineering point of view about fatigue of polymer matrix composite materials. Int J Fatigue 2006;28:1094–9
[15] Owen MJ, Howe RJ. The accumulation of damage in a glass-reinforced plastic under tensile and fatigue loading. J Phys D Appl Phys 1972;5:319
[16] Nouri H, Lubineau G, Traudes D. An experimental investigation of the effect of shear-induced diffuse damage on transverse cracking in carbon-fiber reinforced laminates. Compos Struct 2013;106:529–36
[17] Zhang W, Zhou Z, Zheng P, Zhao S. The fatigue damage mesomodel for fiber-reinforced polymer composite lamina. J Reinf Plast Compos 2014;33:1783–93
[18] Gamstedt EK, Talreja R. Fatigue damage mechanisms in unidirectional carbon-fibre-reinforced plastics. J Mater Sci 1999;34:2535–46
[19] Dong H, Li Z, Wang J, Karihaloo BL. A new fatigue failure theory for multidirectional fiber-reinforced composite laminates with arbitrary stacking sequence. Int J Fatigue 2016;87:294–300
[20] Lasri L, Nouari M, Mansori M El. Wear resistance and induced cutting damage of aeronautical FRP components obtained by machining. Wear 2011;271:2542–8
[21] Lubineau G. Estimation of residual stresses in laminated composites using field measurements on a cracked sample. Compos Sci Technol 2008;68:2761–9

[22] Quaresimin M, Susmel L, Talreja R. Fatigue behaviour and life assessment of composite laminates under multiaxial loadings. Int J Fatigue 2010;32:2–16
[23] Zhang W, Zhou Z, Scarpa F, Zhao S. A fatigue damage meso-model for fiber-reinforced composites with stress ratio effect. Mater Des 2016;107:212–20
[24] Mejlej VG, Osorio D, Vietor T. An Improved Fatigue Failure Model for Multidirectional Fiber-reinforced Composite Laminates under any Stress Ratios of Cyclic Loading. Procedia CIRP 2017;66:27–32
[25] Brunbauer J, Pinter G. Effects of mean stress and fibre volume content on the fatigue-induced damage mechanisms in CFRP. Int J Fatigue 2015;75:28–38
[26] Karbhari VM, Xian G. Hygrothermal effects on high VF pultruded unidirectional carbon/epoxy composites: Moisture uptake. Compos Part B Eng 2009;40:41–9
[27] Alessi S, Pitarresi G, Spadaro G. Effect of hydrothermal ageing on the thermal and delamination fracture behaviour of CFRP composites. Compos Part B Eng 2014;67:145–53
[28] Barjasteh E, Nutt SR. Moisture absorption of unidirectional hybrid composites. Compos Part A Appl Sci Manuf 2012;43:158–64
[29] Mandell JF, Samborsky DD. DOE/MSU composite material fatigue database: Test methods, materials, and analysis. Albuquerque, NM, and Livermore, CA (United States): 1997
[30] Hashin Z, Rotem A. A Fatigue Failure Criterion for Fiber Reinforced Materials. J Compos Mater 1973;7:448–64
[31] Naderi M, Khonsari MM. A comprehensive fatigue failure criterion based on thermodynamic approach. J Compos Mater 2012;46:437–47
[32] Fawaz Z, Ellyin F. Fatigue Failure Model for Fibre-Reinforced Materials under General Loading Conditions. J Compos Mater 1994;28:1432–51
[33] Tai, NH, Ma CCM, Wu SH (1995) Fatigue behaviour of carbon fibre/PEEK laminate composites *Composites*, 26: 551-559
[34] Gamstedt KE, Talreja R (1999) Fatigue damage mechanisms in unidirectional carbon-fibre-reinforced plastics *Journal of Material Science*, 34: 2535-2546
[35] Talreja R (1981) Fatigue of composite materials: damage mechanisms and fatigue-life diagrams *Proc. Roy. Soc. London*, A378: 461-475
[36] Curtis PT (1991) Tensile fatigue mechanisms in unidirectional polymer matrix composite materials *International Journal of Fatigue*, 13: 377-382
[37] Hojo M, Ochiai S, Gustafson CG, Tanaka K, (1994), Effect of matrix resin on delamination fatigue crack growth in CFRP laminates, *Engineering Fracture Mechanics*, 49, 1, 35-47.
[38] Yee A, Modifying Matrix Materials for Tougher Composites, (1987), Toughened Composites, STP937-EB, Johnston N, ASTM International, West Conshohocken, PA, 1987, 383-396.
[39] Mouritz AP (2014), Structural properties of z-pinned carbon-epoxy T-joints in hot-wet environment, *Journal of Composite Materials*, 48, 23, 2905-2914.
[40] Hiremath C, Senthilnathan K, Guha A, Tewari A (2015) Effect of volume fraction on damage accumulation for a lattice arrangement of fibers in CFRP *Materials Today: Proceedings*, 2: 2671-2678
[41] Brunbauder J, Pinter G (2015) Effects of mean stress and fibre volume content on the fatigue-induced damage mechanisms in CFRP *International Journal of Fatigue*, 75: 28-38
[42] Brunbauer J, Stadler H, Pinter G (2015) Mechanical properties, fatigue damage and microstructure of carbon/epoxy laminates depending on fibre volume content *International Journal of Fatigue*,70:85-92
[43] Cali C, Cricri G, Perrella M (2010) An advanced creep model allowing for hardening and damage effects *Strain*, 46, 347-357
[44] Gornet L, Wesphal O, Burtin C, Bailleul JL, Rozycki P, Stainer L (2013) Rapid determination of the high cycle fatigue limit curve of carbon fiber epoxy matrix composite laminates by thermography methodology: tests and finite element simulation. *Procedia Engineering*, 66: 697-704
[45] Peyrac C, Jollivet T, Leray N, Lefebvre F, Westphal O, Gornet L (2015) Self-heating method for fatigue limit determination on thermoplastic composites *Procedia Engineering*, 133: 129-135
[46] Barron V, Buggy M, McKenna NH, (2001), Frequency effects on the fatigue behaviour on carbon fibre reinforced polymer laminates, *Journal of Materials Science*, 36, 7, 1755-1761.
[47] Kharrazi MR, Sarkani S, Frequency-Dependent Fatigue Damage Accumulation in Fiber-Reinforced Plastics, *Journal of Composite Materials*, 35, 21, 1924-1953.
[48] Montesano J, Fawaz Z, Bougherara H (2013) Use of infrared thermography to investigate the fatigue behaviour of carbon fiber reinforced polymer composite *Composite Structures*, 97: 76-83
[49] Crivelli D, Guagliano M, Eaton M, Pearson M, Al-Jumaili S, Holford K, Pullin R (2015) Localisation and identification of fatigue matrix cracking and delamination in a carbon fibre panel by acoustic emission *Composites Part B*, 74: 1-12
[50] Hull D, Clyne TW (1996) An introduction to composite materials (Second Edition), Cambridge, Cambridge University, Cambridge University Press
[51] Broyles NS, Verghese KNE, Davis SV, Lesko JJL, Riffle JS (1998) Fatigue performance of carbon fibre/vinyl ester composites: the effect of two dissimilar polymeric sizing agents *Polymer*, 39: 3417-3424
[52] Deng S, Ye L (1999) Influence of fiber-matrix adhesion on mechanical properties of graphite/epoxy composites: I. Tensile, flexure, and fatigue properties *J. Reinf. Plast. Comp.*, 18: 1021-1040
[53] Tsuchiyama N (1982) In Proc. ICCM-IV Progress in Science and Engineering of Composites, Japan Society for Composite Materials, Tokyo.
[54] Caprino G (2003) Short-fibre thermoset composites. In: Fatigue in Composites, Ed. Harris, B, Elsevier (Woodhead Publishing Imprint) ISBN 978-1-85573-608-5
[55] Hitchen SA, Ogin SL, Smith PA (1995) Effect of fibre length on fatigue of short carbon fibre/epoxy composite *Composites*, 26: 303-308
[56] Harris B, Reither H, Adam T, Dickson RF, Fernando G (1990) Fatigue behaviour of carbon fibre reinforced plastics *Composites*, 21: 232-242
[57] Shutle K, Friedrich K, Horstenkamp G (1986) Temperature-dependent mechanical behaviour of PI and PES resins used as matrices for short-fibre reinforced laminates*Journal of Material Science*, 21: 3561-3570
[58] Zago A, Springer GS (2001) Constant amplitude fatigue of short glass and carbon fiber reinforced thermoplastic*Journal of Reinforced Plastics and Composites*, 20: 564-595
[59] Mandell JF, Huang DD, McGarry FJ (1981) Fatigue of glass and carbon fiber reinforced engineering thermoplastics *Polymer Composites*, 2: 137-144
[60] Pimenta S, Pinho ST (2011) Recycling carbon fibre reinforced polymers for structural applications: Technology review and market outlook *Waste Management*, 31: 378-392
[61] Varna, J.; Joffe, R.; Berglund, L.A.; Lundstrom, T.S. Effect of voids on failure mechanisms in RTM laminates. Compos Sci Technol 1995; 52: 241–249.
[62] Olivier, P.; Cottu, J.P.; Ferret, B. Effects of cure cycle pressure and voids on some mechanical properties of carbon/epoxy laminates. Composites, 1995, 26, 509.
[63] Ruiz, E.; Achim, V.; Soukane, S.; Trochu F.; Breardb J. Optimization of injection flow rate to minimize micro/macro-voids formation in resin transfer molder composites. Compos Sci Technol 2006; 66: 475–486.
[64] Fiedler, B.; and Schulte, K. Reliability and life prediction of composite structures. Compos Sci Technol 2006; 66: 615.
[65] Guo, Z.S.; Liu, L.; Zhang, B.M.; Du, S.; Critical void content for thermoset composite laminates. J Compos Mater 2009; 43: 1775–1790.
[66] Zhang, A.; and Zhang, D. The mechanical property of CFRP laminates with voids. Adv Mater Res 2013; 652–654: 25–28
[67] Liu, L.; Zhang, B.M.; Wang, D.F. Effects of cure cycles on

void content and mechanical properties of composite laminates. Compos Struct 2006; 73: 303–309.
[68] Zangenberg, J. The effects of fibre architecture on fatigue lifetime of composite materials. PhD-Thesis, DTU Wind Energy, 2013.
[69] Sisodia, S.; Gamstedt, E.K.; Edgren, F.; Varna, J. Effects of voids on quasi-static and tension fatigue behaviour of carbon-fibre composite laminates, J. Compos. Mater. 49 (2015) 2137–2148.
[70] Horrmann, S.; Adumitroaie, A.; Viechtbauer, C.; Schagerl M. The effect of fiber waviness on the fatigue life of CFRP materials. Int J Fatigue 2016;90:139–47.
[71] Nonn, S.; Kralovec, C.; Schagerl, M. Damage mechanisms under static and fatigue loading at locally compacted regions in a high pressure resin transfer molded carbon fiber non-crimp fabric. Compos Part A Appl Sci Manuf 2018;115:57–65.
[72] Leclerc, J.S.; and Ruiz, E. Porosity reduction using optimized flow velocity in resin transfer molding. Compos Part A 2008; 39: 1859–1868.
[73] Zhu, H.; Wu, B.; Li, D.; Zhang, D.; Chen, Y. Influence of voids on the tensile performance of carbon/epoxy fabric laminates. J Mater Sci Technol 2011; 27: 69–73.
[74] Costa, M.L.; Rezende, M.C.; Almeida, S.F.M. Influence of porosity on the interlaminar shear strength of carbon/epoxy and carbon/bismaleimide fabric laminates. J. Composite Sci. Technol. 2001, 61, 2101 – 2108.
[75] de Almeida, S.F.M.; and dos Santos Nogueira Neto Z. Effect of void content on the strength of composite laminates. Compos Struct 1994; 28: 139–148.
[76] Koissin, V.; Kustermans, J.; Lomov, S.V.; Verpoest, I.; Van Den Broucke, B.; Witzel, V. Structurally stitched NCF preforms: quasi-static response. Compos Sci Technol 2009; 69: 2701–2710.
[77] Huang, Y.; Varna, J.; Talreja, R. Statistical methodology for assessing manufacturing quality related to transverse cracking in cross ply laminates. Compos. Sci. Technol, 2014, 95, 100–106.
[78] Carraro, P.A.; Maragoni, L.; Quaresimin, M. Influence of manufacturing induced defects on damage initiation and propagation in carbon/epoxy NCF laminates. Adv Manuf Polym Compos Sci 2015;1:44–53.
[79] Wisnom, M.R.; Reynolds, T.; Gwilliam, N. Reduction in interlaminar shear strength by discrete and distributed voids, Composites Science and Technology, vol.56, issue.1, pp.93-101, 1996.
[80] Zhu, H.Y.; Li, D.H.; Zhang, D.X.; Wu, B.; Chen, Y. Influence of voids on interlaminar shear strength of carbon/epoxy fabric laminates. Trans Nonferrous Metals Soc China 2009; 19: 470–475.
[81] Suhot, M.A.; Chambers, A.R. The effect of voids on the flexural fatigue performance of unidirectional carbon fibre composites Proc. ICCM16, Kyoto, Japan, July 2007.
[82] Rotem, A.; and Nelson H.G. Failure of a laminated composite under tension-compression fatigue loading. Compos Sci Technol 1989; 36: 45–62.
[83] Chambers, A.R.; Earl, J.S.; Squires, C.S.; Suhot, M.A. The effect of voids on the flexural fatigue performance of unidirectional carbon fibre composites developed for wind turbine applications. Int J Fatigue 2005; 28: 1389–1398.
[84] Gehrig, F.; Mannov, E.; Schulte, K. Degradation of NCF-epoxy composites containing voids. Proc. ICCM 17, July 2009.
[85] Seon, G.; Makeev, A.; Nikishkov, Y.; Lee, E. Effects of defects on interlaminar tensile fatigue behavior of carbon/epoxy composites, Compos. Sci. Technol. 89 (2013) 194–201.
[86] Parlevliet, P.P.; Bersee,H.E.N.; Beukers, A. Measurement of (post-)curing strain development with fibre Bragg gratings, Polym. Test. 29 (2010) 291–301.
[87] Tavakol, B.; Roozbehjavan, P.; Ahmed, A.; Das, R.; Joven, R.; Koushyar, H.; Rodriguez, A.; Minaie, B. Prediction of residual stresses and distortion in carbon fiber-epoxy composite parts due to curing process using finite element analysis, J. Appl. Polym. Sci. 128 (2013) 941–950.
[88] Mesogitis, T.S.; Skordos, A.A.; Long, A.C. Uncertainty in the manufacturing of fibrous thermosetting composites: A review, Compos. Part A Appl. Sci. Manuf. 57 (2014) 67–75.
[89] Hosoi, A.; and Kawada, H. Fatigue Life Prediction for Transverse Crack Initiation of CFRP Cross-Ply and Quasi-Isotropic Laminates, Materials (Basel). 11 (2018) 1182.
[90] Padmanabhan, S.K.; Pitchumani, R. Stochastic analysis of isothermal cure of resinsystems. Polym Compos 1999;20(1):72–85
[91] Guo, Z.; Du, S.; Zhang, B. Temperature field of thick thermoset composite laminates during cure process. Compos Sci Technol 2005;65(3–4):517–23.
[92] Potter, K.; Khan, B.; Wisnom, M.; Bell, T.; Stevens, J. Variability, fibre waviness and misalignment in the determination of the properties of composite materials and structures. Compos Part A: Appl Sci Manuf 2008;39(9):1343–54.
[93] Potter K. Understanding the origins of defects and variability in composites manufacture. In: International conference on composite materials (ICCM)-17, Edinburgh, UK; 2009.
[94] Horrmann, S.; Adumitroaie, A.; Schagerl M. The effect of ply folds as manufacturing defect on the fatigue life of CFRP materials. Frat Ed Integrita Strutt 2016;10:76–81.
[95] Mukhopadhyay, S.; Jones, M.I.; Hallett, S.R. Compressive failure of laminates containing an embedded wrinkle; experimental and numerical study. Compos Part A: Appl Sci Manuf 2015;73:132–42.
[96] Davidson, P.; Waas A.M.; Yerramalli, C.S.; Chandraseker, K.; Faidi W. Effect of fiber waviness on the compressive strength of unidirectional carbon fiber composites. In: 53rd AIAA/ASME/ASCE/AHS/ASC structures, structural dynamics and materials conference, AIAA 2012-1612, Honolulu, Hawaii; 2012.
[97] Wang, J.; Potter, K.; Etches, J. Experimental investigation and characterisation techniques of compressive fatigue failure of composites with fibre waviness at ply drops. Compos Struct 2013;100:398–403.
[98] Horrmann, S.; Viechtbauer, C.; Adumitroaie, A.; Schagerl, M. The effect of fiber waviness as manufacturing defect on the fatigue life of CFRP materials. In: ICCM20, Copenhagen, Denmark; 2015.
[99] Konur O, Matthews FL, (1989), *Effect of the properties of the constituents on the fatigue performance of composites: a review*, Composites, 20, 4, 317-328.
[100] Jones CJ, Dickson RF, Adam T, Reiter H, Harris B, (1984), *The environmental fatigue behaviour of reinforced plastics*, Proc Royal Soc London A, 369, 315-338.
[101] Curtis PT, Moore BB, (1983), A comparison of plain and double waisted coupons for static and tensile testing of UD GRP and CFRP, *Second International Conference on Composite Structures*, Paisley, Scotland, UK, September 1983, Proceedings (Elsevier Applied Science Publishers, London, UK, 383-398.
[102] Casas-Rodriguez JP, Ashcroft IA, Silberschmidt VV (2008) Delamination in adhesively bonded CFRP joints: Standard fatigue, impact-fatigue and intermittent impact *Composites Science and Technology*, 68: 2401-2409
[103] Nash NH, Young TM, McGrail PT, Stanley WF (2015) Inclusion of a thermoplastic phase to improve impact and post-impact performances of carbon fibre reinforced thermosetting composites - a review *Materials and Design*, 85: 582-597
[104] Kempf M, Schwagele S, Ferencz A, Altstadt V (2011) Effect of impact damage on the compression fatigue performance of glass and carbon fibre reinforced composites *18th International Conference on Composites Materials (ICCM)*, 21th to 26th of August, 2011, Jeju Island, Korea
[105] Alam P (2018) Structures and composition of the crab carapace – an archetypal material in biomimetic mechanical design *Results and Problems in Cell Differentiation*, pp 569-584, Ed. Kloc, M. Springer-Nature
[106] Tai NH, Ma CCM, Lin JM, Wu GY (1999) Effects of thickness on the fatigue-behaviour of quasi-isotropic carbon/epoxy composites before and after low energy impacts *Composites Science and Technology*, 59: 1753-1762

[107] Nettles A, Hodge A, Jackson J (2011) An examination of the compressive cyclic loading aspects of damage tolerance for polymer matrix launch vehicle hardware *Journal of Composite Materials*, 45: 437-458

[108] Cantwell W, Curtis P, Morton J (1983) Post-impact fatigue performance of carbon fibre laminates with non-woven and mized-woven layers *Composites*, 14: 301-305

[109] Melin LG, Schon J (2001) Buckling behaviour and delamination growth in impacted composite specimens under fatigue load: an experimental study *Composites Science and Technology*, 61: 1841-1852

[110] Beheshty MH, Harris B (1998) A constant-life model of fatigue behaviour for carbon-fibre composites: the effect of impact damage *Composites Science and Technology*, 58: 9-18

[111] Mitrovic M, Hahn HT, Carman GP, Shyprykevich P (1999) Effect of loading parameters on the fatigue behaviour of impact damaged composite laminates *Composites Science and Technology*, 59: 2059-2078

[112] Malin LG, Schon J (2001) Buckling behaviour and delamination growth in impacted composite specimens under fatigue load: an experimental study *Composites Science and Technology*, 61: 1841-1852

[113] Ogasawara T, Sugimoto S, Katoh H, Ishikawa T (2013) Fatigue behaviour and lifetime distribution of impact-dmaged carbon fibre/toughened epoxy composites under compressive loading *Advanced Composite Materials*, 22: 65-78

[114] Saito H, Kimpara I (2006) Evaluation of impact damage mechanism of multi-axial stiched CFRP laminate *Composites Part A: Applied Science and Manufacturing*, 37: 2226-2235

[115] Saito H, Kimpara I (2009) Damage evolution behaviour of CFRP laminates under post-impact fatigue with water absorption environment *Composites Science and Technology*, 69: 847-855

[116] Im KH, Cha CS, Kim SK, Yang IY (2001) Effects of temperature on impact damage in CFRP composite laminates *Composites Part B: Engineering*, 32: 669-682

[117] Uda N, Ono K, Kunoo K (2009) Compression fatigue failure of CFRP laminates with impact damage *Composites Science and Technology*, 69: 2308-2314

[118] Kostopoulos V, Baltopoulos A, Karapappas P, Vavouliotis A, Paipetis A (2010) Impact and after-impact properties of carbon fibre reinforced composites enhanced with multi-wall carbon nanotubes *Composites Science and Technology*, 70: 553-563

[119] Koo JM, Choi JH, Seok CS (2014) Prediction of post-impact residual strength and fatigue characteristics after impact of CFRP composite structures *Composites Part B: Engineering*, 61: 300-306

[120] Symons DD, Davis G (2000) Fatigue testing of impact-damaged T300/914 carbon-fibre-reinforced plastic *Composites Science and Technology*, 60: 379-389

[121] Freeman B, Schwingler E, Mahinfalah M, Kellogg K (2005) the effect of low-velocity impact on the fatigue life of sandwich composites *Composites Structures*, 70: 374-381

[122] Tai NH, Ma CCM, Lin JM, Wu GY (1999) Effects of the thickness on the fatigue-behaviour of quasi-isotropic carbon/epoxy composites before and after low energy impacts *Composites Science and Technology*, 59: 1753-1762

[123] Campbell, F. C. (2003). Manufacturing Processes for Advanced Composites. *Manufacturing Processes for Advanced Composites*.

[124] Quaresimin, M., Ricotta, M. (2015) Fatigue response and damage evolution in 2D textile composites, *Fatigue of Textile Composites*, Woodhead Publishing, Pages 193-221.

[125] Bishop, S. M. (1989). Strength and failure of woven carbon-fibre reinforced plastics for high performance applications. In T.-W. Chou, F. K. Ko (Eds.), *Textile structural composites* (pp. 173e207). Amsterdam: Elsevier.

[126] Sevenois, R. D. B., Van Paepegem, W. (2015). Fatigue Damage Modeling Techniques for Textile Composites: Review and Comparison With Unidirectional Composite Modeling Techniques. *Applied Mechanics Reviews*, 67(2), 21401.

[127] Daggumati, S., De Baere, I., Van Paepegem, W., Degrieck, J., Xu, J., Lomov, S. V., Verpoest, I. (2013). Fatigue and post-fatigue stress-strain analysis of a 5-harness satin weave carbon fibre reinforced composite. *Composites Science and Technology*.

[128] Gyekenyesi AL (1998). Isothermal fatigue, damage accumulation, and life prediction of a woven PMC. *NASA/1998-206593*; .

[129] Kawai, M., Taniguchi, T. (2006). Off-axis fatigue behavior of plain weave carbon/epoxy fabric laminates at room and high temperatures and its mechanical modeling. *Composites Part A: Applied Science and Manufacturing*.

[130] Pandita, S. D., Huysmans, G., Wevers, M., Verpoest, I. (2001). Tensile fatigue behaviour of glass plain-weave fabric composites in on- and off-axis directions. *Composites - Part A: Applied Science and Manufacturing*.

[131] Fruehmann, R. K., Dulieu-Barton, J. M., Quinn, S. (2010). Assessment of fatigue damage evolution in woven composite materials using infra-red techniques. *Composites Science and Technology*.

[132] Pandita, S. D., Verpoest, I. (2004). Tension-tension fatigue behaviour of knitted fabric composites. *Composite Structures*.

[133] Kelkar, A. D., Tate, J. S., Bolick, R. (2006). Structural integrity of aerospace textile composites under fatigue loading. *Materials Science and Engineering B: Solid-State Materials for Advanced Technology*.

[134] Tate, J. S., Kelkar, A. D., Whitcomb, J. D. (2006). Effect of braid angle on fatigue performance of biaxial braided composites. *International Journal of Fatigue*

[135] J. Montesano, Z. Fawaz, C. Poon, K. Behdinan, (2014) A microscopic investigation of failure mechanisms in a triaxially braided polyimide composite at room and elevated temperatures,*Materials and Design*, 53.

[136] Dransfield K, Baillie C, Mai Y-W, (1994) Improving the delamination resistance of CFRP by stitching, *Composites Science and technology*, 50,305-317.

[137] Mouritz AP, Bannister MK, Falzon PJ, Leong KH, (1999) Review of applications for advanced three-dimensional fibre textile composites, *Composites Part A: Applied Science and Manufacturing*, 30, 12, 1445-1461.

[138] Bogdanovich AE, Mohamed MH, (2009), Three-dimensional reinforcement for composites, *SAMPE Journal*, 45, 8-28.

[139] Mouritz AP, (2015), Fatigue of 3D textile-reinforced composites, Chapter 11 in Fatigue of Textile Composites, Woodhead Publishing Series *Composites Science and Engineering*, 255-274.

[140] Mouritz AP, Baini C, Herszberg I, (1999), Mode I interlaminar fracture toughness properties of advanced textile fibreglass composites, *Composites Part A: Applied Science and Manufacturing*, 30, 7, 859-870.

[141] Gerlach R, Siviour CR, Wiegand J, Petrinic N, (2012), In-plane and through-thickness properties, failure modes, damage and delamination in 3D woven carbon fibre composites subjected to impact loading, *Composites Science and Technology*, 72, 3, 397-411.

[142] Mouritz AP, Cox BN, (2010), A mechanistic interpretation of the comparative in-plane mechanical properties of 3D woven, stitched and pinned composites, *Composites Part A: Applied Science and Manufacturing*, 41, 6, 709-728.

[143] Aymerich F, (2004), Effect of Stitching on the Static and Fatigue Performance of Co-Cured Composite Single-Lap Joints, *Journal of Composite Materials*, 38, 3, 243-257.

[144] Aymerich F, Priolo P, (2003), Sun CT, Static and fatigue behaviour of stitched graphite/epoxy composite laminates, *Composites Science and Technology*, 63, 6, 907-917.

[145] Chang P, Mouritz AP, Cox BN, (2007), Flexural properties of z-pinned laminates, *Composites Part A: Applied Science and Manufacturing*, 38, 2, 244-251.

[146] Chang P, Mouritz AP, Cox BN, (2006), Properties and failure mechanisms of z-pinned laminates in monotonic and cyclic tension, *Composites Science and Technology*, 37, 10, 1501-1513.

[147] Carvelli V, Tomaselli VN, Lomov SV, Verpoest I, Witzel V,

Van den Broucke B, (2010) Fatigue and Post-Fatigue tensile behaviour of Non-Crimp stitched and unstitched Carbon/Epoxy composites, *Composites Science and Technology*, 70, 15, 2216-2224.

[148] Rudov-Clark S, Mouritz AP, (2008), Tensile fatigue properties of a 3D orthogonal woven composite, *Composites Part A*, 39, 1018-1024.

[149] Tong L, Mouritz AP, Bannister MK, (2002), 3D fibre reinforced polymer composites, *Oxford: Elsevier*.

[150] Tana KT, Watanabe N, Iwahori Y, Effect of stitch density and stitch thread thickness on low-velocity impact damage of stitched composites, (2010), *Composites Part A: Applied Science and Manufacturing*, 41, 12, 1857-1868.

[151] Dransfield KA, Jain LK, Mai YW, (1998), On the effects of stitching in CFRPs—I. mode I delamination toughness, *Composites Science and Technology*, 58, 6, 815-827.

[152] Lopresto V, Melito V, Leone C, Caprino G, (2006), Effect of stitches on the impact behaviour of graphite/epoxy composites, *Composites Science and Technology*, 66, 2, 206-214.

[153] Mouritz AP, Cox BN, (2000), A mechanistic approach to the properties of stitched laminates, *Composites Part A*, 31, 1-27.

[154] Yudhanto A, Watanabe N, Iwahori Y, Hoshi H, (2014), Effect of stitch density on fatigue characteristics and damage mechanisms of stitched carbon/epoxy composites, *Composites Part A: Applied Science and Manufacturing*, 60, 5, 52-65.

[155] Freitas G, Magee C, Dardzinski P, Fusco T, (1994), Fibre insertion process for improved damage tolerance in aircraft laminates, *Journal of Advanced Materials*, 25, 36-43.

[156] Isa MD, Feih S, Mouritz AP, (2011), Compression fatigue properties of quasi-isotropic z-pinned carbon/epoxy laminate with barely visible impact damage, *Composite Structures*, 93, 2222-2230.

[157] Kelkar AD, Tate JS, Bolick R, (2006), Structural integrity of aerospace composites under fatigue loading, *Materials Science and Engineering B*, 132, 79-84.

[158] Bilisik K, (2013), Three-dimensional braiding for composites: a review, *Textile Research Journal*, 83, 13, 1414–1436.

[159] Carvelli V, Pazmino J, Lomov SV, Bogdanovich AE, Mungalov DD, Verpoest I, (2012) Quasi-static and fatigue tensile behavior of a 3D rotary braided carbon/epoxy composite, *Journal of Composite Materials*, 47, 25, 3195–3209.

[160] Curtis G, Milne J, Reynolds W, (1968), Non-Hookean behaviour of strong carbon fibres, *Nature*, 220, 1024-1025.

[161] Carvelli V, Lomov SV, (2015), Fatigue damage evolution in 3D textile composites, Chapter 10 in Fatigue of Textile Composites, Woodhead Publishing Series in *Composites Science and Engineering*, 223-253.

[162] Pingkarawat K, Mouritz AP, (2014), Improving the mode I delamination fatigue resistance of composites using z-pins, *Composites Science and Technology*, 92, 70-76.

[163] Tan KT, Watanabe N, Iwahori Y, Ishikawa T, (2011), Influence of Stitch Density and Stitch Thread Thickness on Compression After Impact Strength of Stitched Composites, *16th International Conference on Composite Structures*, ICCS 16, Porto.

[164] Tong L, Jain LK, Leong KH, Kelly D, Hertzberg I, (1998), Failure of transversely stitched RTM lap joints, *Composites Science and Technology*, 58, 221-227.

[165] McCarthy MA, McCarthy CT, Lawlor VP, Stanley WF, (2005) Three-dimensional finite element analysis of single-bolt, single-lap composite bolted joints: part I—model development and validation, *Composite Structures*, 71, 2, 140-158.

[166] O'Higgins RM, McCarthy MA, McCarthy CT, (2008) Comparison of open hole tension characteristics of high strength glass and carbon fibre-reinforced composite materials, *Composites Science and Technology*, 68, 13, 2770-2778.

[167] Dai S, Cunningham PR, Marshall S, Silva C, (2015), Open hole quasi-static and fatigue characterization of 3D woven composites, *Composite Structures*, 131, 765-774.

[168] Yudhanto A, Iwahori Y, Watanabe N, Hoshi H, (2012), Open hole fatigue characteristics and damage growth of stitched plain weave carbon/epoxy laminates, *International Journal of Fatigue*, 43, 12-22.

[169] Diamantakos C, Fritz RJ, (1988), Tensile Fatigue of Notched Carbon/Epoxy Specimens Search for Optimum Model, *Journal of Reinforced Plastics and Composites*, 7, 165-178.

[170] Vieille B, (2018), Fatigue accumulated damage in notched quasi-isotropic composites under high-temperature conditions: A discussion on the influence of matrix nature on the stress energy release rate, *Journal of Composite Materials*, 52, 17, 2397-2412.

[171] Tsai KH, Chiu CH, Wu TH, (2000), Fatigue behavior of 3D multi-layer angle interlock woven composite plate, *Composites Science and Technology*, 60, 2, 241-248.

[172] Sudarsono S, Oji K, (2017), Fatigue Behavior of Open-Holed CFRP Laminates with Initially Cut Fibers, *Open Journal of Composite Materials*, 7, 49-62.

[173] Fernandez G, Usabiaga H, Vandepitte D, (2017), Subcomponent development for sandwich composite wind turbine blade bonded joints analysis, *Composite Structures*, 180, 11, 41-62.

[174] Alam P, Robert C, Ó Brádaigh CM (2018) Tidal turbine blade composites - a review on the effects of hygrothermal aging on the perties of CFRP. Composites Part B: Engineering, 149: 248-259

[175] Sauder C, Lamon J, Pailler R (2002) Thermomechanical properties of carbon fibres at high temperatures (up to 2000°C). Composites Science and Technology, 62: 499-504

[176] Pradere C, Batsale JC, Goyheneche JM, Pailler R, Dilhaire S (2009) Thermal properties of carbon fibers at very high temperature. Carbon, 47: 737-743

[177] Daniel IM, Liber T (1975) Lamination residual stresses in fiber composites. Interim report NASA CR-134826, IITRI D6073-I

[178] Fahmy A, Cunningham TG (1976) Investigation of thermal fatigue in fiber composite materials. Final report, NASA CR-2641

[179] Givler RC, Gillespie JW, Pipes RB (1982) Environmental exposure of carbon/epoxy composite material systems. ASTM STP 768: Composites for Extreme Environments

[180] Camahort JL, Rennhack EH, Coons WC (1976) Effects of thermal cycling environment on graphite/epoxy composites. ASTM STP 602: Environmental Effects on Advanced Composite Materials

[181] Eselun SA, Neubert HD, Woff EG (1979) Microcracking effects on dimensional stability. SAMPE Journal, 24 :1299-1309

[182] Adams DS, Bowles DE, Herakovich CT (1986) Thermally induced transverse cracking in graphite/epoxy cross-ply laminates. Journal of Reinforced Plastics and Composites, 5: 152-169

[183] Hyer MW, Cooper DW, Cohen D (1986) Stresses and deformations in cross-ply composite tubes subjected to a uniform temperature change. Journal of Thermal Stresses, 9: 97-117

[184] Kaw AK (1997) Mechanics of Composite Materials. CRC Press, New York

[185] Miyano Y, Nakada M, Kudoh H, Muki R (1999) Prediction of tensile fatigue life under temperature environment for unidirectional CFRP. Advanced Composite Materials, 8: 235-246

[186] Miyano Y, Nakada M (2012) Formulation of time- and temperature- dependent strength of unidirectional carbon fiber reinforced plastics. Journal of Composite Materials, 47: 1897-1906

[187] Peters PWM Andersen SI(1988) The influence of matrix fracture strain and interface strength on cross ply cracking in CFRP in the temperature range of -100°C to +100°C. Journal of Composite Materials, 23: 944-960

[188] Grogan DM, Leen SB, Semprimoschnig COA, Ó Brádaigh CM (2014) Damage Characterisation of Cryogenically Cycled Carbon/PEEK Laminates. Composites Part A: Applied Science and Manufacturing, 66: 237-250

[189] Miyano Y, McMurray MK, Ktade N, Nakada M (1995) Loading rate and temperature dependence of flexural behaviour of unidirectional pitch-based CFRP laminates. Composites, 26: 713-717

[190] Kawai M, Taniguchi T (2006) Off-axis fatigue behavior of plain weave carbon/epoxy fabric laminates at room temperatures and

its mechanical modeling. Composites Part A: Applied Science and Manufacturing, 37: 243-256
[191] Khan RKZ, Al-Sulaiman F, Merah N (2002) Fatigue life estimates in woven carbon fabric/epoxy composites at non-ambient temperatures. Journal of Composite Materials, 36: 2517-2535
[192] Wu CML (1993) Thermal and mechanical fatigue analysis of CFRP laminates. Composite Structures, 25: 339-344
[193] Kobayashi S, Terada K, Takeda N (2003) Evaluation of long-term durability in high temperature resistant CFRP laminates under thermal fatigue loading. Composites Part B: Engineering, 34: 753-759
[194] Henaff-Gardin C, Lafarie-Frenot MC (2002) Specificity of matrix-cracking development in CFRP laminates under mechanical or thermal loadings. International Journal of Fatigue, 24: 171-177
[195] Miyano Y, Nakada M (2006) Time and temperature dependent fatigue strengths for three directions of unidirectional CFRP. Experimental Mechanics, 46: 155-162
[196] Kawai M, Maki N (2006) Fatigue strengths of cross-ply CFRP laminates at room and high temperatures and its phenomenological modeling. International Journal of Fatigue, 28: 1297-1306
[197] Miyano Y, Nakada M, Judoh H, Muki R (2000) Prediction of tensile fatigue life for unidirectional CFRP. Journal of Composite Materials, 34: 538-550
[198] Miyano Y, Nakada M, Muki R (1999) Applicability of fatigue life prediction method to polymer composites. Mechanics of Time Dependent Materials, 3: 141-157
[199] Vanlandingham MR, Eduljee RF, Gillespie JR (1999) Moisture diffusion in epoxy systems. Journal of Applied Polymer Science, 71: 787-798
[200] Barrer RM (1941) Diffusion in and through solids. New York, The Macmillan Company Cambridge England: University Press
[201] Gac PYL, Arhant M, Gall ML, Davies P (2017) Yield stress changes induced by water in polyamide 6: characterisation and modelling. Polymer Degradation and Stability, 272-280
[202] Judd NCW (1977) Absorption of water into carbon fibre composites. The British Polymer Journal, March 1977, 36-40
[203] Karbhari VM, Xian G (2009) Hygrothermal effects on high V_F pultruded unidirectional carbon/epoxy composites: moisture uptake. Composites: Part B, 40: 41-49
[204] Dellanno G, Lees R (2012) Effect of water immersion on the interlaminar and flexural performance of low cost liquid resin infused carbon fabric composites. Composites: Part B, 43, 1368-1373
[205] Wang Y, Hahn TH (2007) AFM characterisation of the interfacial properties of carbon fibre reinforced polymer composites subjected to hygrothermal treatments. Composites Science and Technology, 67: 92-101
[206] Collings TA, Stone DEW (1985) Hygrothermal effects in CFRP laminates: strains induced by temperature and moisture. Composites, 16: 307-316
[207] Selzer R, Friedrich K (1997) Mechanical properties and failure behaviour of carbon fibre-reinforced polymer composites under the influence of moisture. Composites: Part A, 28A: 595-604
[208] Nakai Y, Hiwa C (2002) Effects of loading frequency and environment on delamination fatigue crack growth of CFRP. International Journal of Fatigue, 24: 161-170
[209] Matsuda S, Hojo M, Ochiai S (1999) Effect of water environment on mode II delamination fatigue in interlayer-toughened CFRP. JSME International Journal, 42: 421-428
[210] Komai K, Minoshima K, Shibutani T, Nomura T (1989) The influence of water on the mechanical properties and fatigue strength of angle-ply carbon/epoxy composites. JSME International Journal, 32: 588-595
[211] Kawada H, Kobiki A, Koyanagi J, Hosoi A (2005) Long-term durability of polymer matrix composites under hostile environments. Materials Science and Engineering A, 412: 159-164
[212] Chiou P, Bradley WL (1995) Effects of seawater absorption on fatigue crack development in carbon/epoxy EDT specimens. Composites, 26: 869-876
[213] Hojo M, Tanaka K, Gistafson CG, Hayashi R (1989) Propagation of delamination fatigue cracks in CFRP in water. JSME International Journal, 32: 292-299
[214] Dickinson RF, Jones CJ, Harris B, Leach DC, Moore DR (1985) The environmental fatigue behaviour of carbon fibre reinforced polyether ether ketone. Journal of Materials Science, 20: 60-70
[215] Meziere Y, Bunsell AR, Favry Y, Teissedre JC, Do AT (2005) Large strain cyclic fatigue testing of unidirectional carbon fibre reinforced epoxy resin. Composites Part A: Applied Science and Manufacturing, 36: 1627-1636
[216] Kawai M, Yagihashi Y, Hoshi H, Iwahori Y (2013) Anisomorphic constant fatigue life diagrams for quasi-isotropic woven fabric carbon/epoxy laminates under different hygrothermal environments. Advanced Composite Materials, 22: 79-98
[217] Zhang A, Lu H, Zhang D (2014) Synergistic effect of cyclic mechanical loading and moisture absorption on the bending fatigue performance of carbon/epoxy composites. Journal of Materials Science, 49: 314-320
[218] Guen-Geffroy AL, Gac PYL, Diakhate M, Habert B, Davies P (2018) Lon-term durability of CFRP under fatigue loading for marine applications. MATEC Web of Conferences: Fatigue 2018, 165: 07001[2018]
[219] Stinchbomb WW; Bakis CE. Fatigue Behavior of Composite Laminates. Compos Mater Ser 1991;4:105–80
[220] Quaresimin M, Ricotta M. Fatigue behaviour and damage evolution of single lap bonded joints in composite material. Compos Sci Technol 2006;66:176–87
[221] May M, Hallett SR. An advanced model for initiation and propagation of damage under fatigue loading – part I: Model formulation. Compos Struct 2011;93:2340–9
[222] May M, Hallett SR. Damage initiation in polymer matrix composites under high-cycle fatigue loading – A question of definition or a material property? Int J Fatigue 2016;87:59–62
[223] Paris P, Erdogan F. A Critical Analysis of Crack Propagation Laws. J Basic Eng 1963;85:528
[224] Corten HT. Composite Materials: Testing and Design (Second Conference). ASTM International; 1972
[225] DorMohammdi S, Godines C, Abdi F, Huang D, Repupilli M, Minnetyan L. Damage-tolerant composite design principles for aircraft components under fatigue service loading using multi-scale progressive failure analysis. J Compos Mater 2017;51:2181–202
[226] O'Brien T, editor. Long-Term Behavior of Composites. 100 Barr Harbor Drive, PO Box C700, West Conshohocken, PA 19428-2959: ASTM International; 1983
[227] Shivakumar K, Chen H, Abali F, Le D, Davis C. A total fatigue life model for mode I delaminated composite laminates. Int J Fatigue 2006;28:33–42
[228] Holmes JW, Liu L, Sørensen BF, Wahlgren S. Experimental approach for mixed-mode fatigue delamination crack growth with large-scale bridging in polymer composites. J Compos Mater 2014;48:3111–28
[229] Khan R, Alderliesten R, Yao L, Benedictus R. Crack closure and fibre bridging during delamination growth in carbon fibre/epoxy laminates under mode I fatigue loading. Compos Part A Appl Sci Manuf 2014;67:201–11
[230] Yao L, Alderliesten R, Zhao M, Benedictus R. Bridging effect on mode I fatigue delamination behavior in composite laminates. Compos Part A Appl Sci Manuf 2014;63:103–9
[231] Kawai M. A phenomenological model for off-axis fatigue behavior of unidirectional polymer matrix composites under different stress ratios. Compos Part A Appl Sci Manuf 2004;35:955–63
[232] Petermann J, Schulte K. The effects of creep and fatigue stress ratio on the long-term behaviour of angle-ply CFRP. Compos Struct 2002;57:205–10
[233] Reis PNB, Ferreira JAM, Costa JDM, Richardson MOW. Fatigue life evaluation for carbon/epoxy laminate composites under constant and variable block loading. Compos Sci Technol 2009;69:154–60
[234] Kawai M, Yang K, Oh S. Effect of alternating R-ratios load-

ing on fatigue life of woven fabric carbon/epoxy laminates. J Compos Mater 2015;49:3387–405
[235] Sturgeon JB. Creep, repeated loading, fatigue and crack growth in +/ − 45 oriented carbon fibre reinforced plastics. J Mater Sci 1978;13:1490–8
[236] Gude M, Hufenbach W, Koch I, Koschichow R, Schulte K, Knoll J. Fatigue Testing of Carbon Fibre Reinforced Polymers under VHCF Loading. Procedia Mater Sci 2013;2:18–24
[237] Noda J, Nakada M, Miyano Y. Fatigue Life Prediction under Variable Cyclic Loading Based on Statistical Linear Cumulative Damage Rule for CFRP Laminates. J Reinf Plast Compos 2007;26:665–80
[238] Irving C, Archer E, PE S. Polymer Composites in the Aerospace Industry. vol. Number 50. Elsevier Science, 2014
[239] Harris, B.; Reiter, H.; Adam, T.; et al. Fatigue behaviour of carbon fibre reinforced plastics. Composites 1990; 21(3): 232–242.
[240] Harris, B.; Gathercole, N.; Lee, J.A, et al. Life-prediction for constant-stress fatigue in carbon-fibre composites. Philos Trans Roy Soc Lond 1997; A355: 1259–1294.
[241] Adam, T.; Gathercole, N.; Reiter, H.; et al. Fatigue life prediction for carbon fibre composites. Adv Compos Lett 1992; 1: 23–26.
[242] Gathercole, N.; Reiter, H.; Adam, T.; et al. Life prediction for fatigue of T800/5245 carbon-fibre composites: I. constant-amplitude loading. Fatigue 1994; 16: 523–532.
[243] Beheshty, M.H.; and Harris, B.A. constant-life model of fatigue behavior for carbon-fibre composites: The effect of impact damage. Compos Sci Technol 1998; 58: 9–18.
[244] Kawai, M. Fatigue life prediction of composite materials under constant amplitude loading. In: Vassilopoulos AP (ed.) Fatigue life prediction of composites and composite structures. Cambridge, UK: Woodhead Publishing Limited, 2010, pp.177–219.
[245] Kawai M. Fatigue of composites—life prediction methods. In: Nicolais L and Borzacchiello A (eds) Encyclopedia of composites. Volume 2, 2nd ed. Hoboken, NJ: John Wiley and Sons, 2012, pp.883–923.
[246] Goodman, J. Mechanics applied to engineering. Harlow, UK: Longman Green, 1899.
[247] Harris, B.; Gathercole, N.; Lee J.A.; et al. Life-prediction for constant-stress fatigue in carbon-fibre composites. Philos Trans Roy Soc Lond 1997; A355: 1259–1294.
[248] Kawai, M.; and Koizumi, M. Nonlinear constant fatigue life diagrams for carbon/epoxy laminates at room temperature. Composites Part A: Applied Science and Manufacturing 2007; 38: 2342–2353.
[249] Kawai, M.; and Murata, T. A three-segment anisomorphic constant life diagram for the fatigue of symmetric angle-ply carbon/epoxy laminates at room temperature. Composites Part A: Applied Science and Manufacturing 2010; 41: 1498–1510.
[250] Kawai, M.; and Matsuda, Y. Anisomorphic constant fatigue life diagrams for a woven fabric carbon/epoxy laminate at different temperatures. Composites Part A: Applied Science and Manufacturing 2012; 43: 647–657.
[251] Kawai, M.; Matsuda, Y.; and Yoshimura, R. A general method for predicting temperature-dependent anisomorphic constant fatigue life diagram for a woven fabric carbon/epoxy laminate. Composites Part A: Applied Science and Manufacturing 2012; 43: 915–925.
[252] Kawai, M.; Yagihashi, Y.; Hoshi, H.; and Iwahori, Y. Anisomorphic constant fatigue life diagrams for quasi-isotropic woven fabric carbon/epoxy laminates under different hygro-thermal environments. Advanced Composite Materials 2013; 22: 79–98.
[253] Kawai, M.; and Itoh, N. A failure-mode based anisomorphic constant life diagram for a unidirectional carbon/epoxy laminate under off-axis fatigue loading at room temperature. Journal of Composite Materials 2014; 48: 571–592.
[254] Kawai, M.; and Yano, K. Anisomorphic constant fatigue life diagrams of constant probability of failure and prediction of P–S–N curves for unidirectional carbon/epoxy laminates. Composites Part A: Applied Science and Manufacturing 2016; 83: 323–334.
[255] Kawai, M.; and Yano, K. Probabilistic anisomorphic constant fatigue life diagram approach for prediction of P–S–N curves for woven carbon/epoxy laminates at any stress ratio. Composites Part A: Applied Science and Manufacturing 2016; 80: 244–258
[256] Vassilopoulos, A.P.; Keller T. Experimental Characterization of Fiber-Reinforced Composite Materials, 2011, p. 25–67.
[257] Hashin Z. Failure criteria for unidirectional fiber composites. J Appl Mech 1980;47:329–34.
[258] Goto K, Arai M, Nishimura M, Dohi K. Strength evaluation of unidirectional carbon fiber-reinforced plastic laminates based on tension–compression biaxial stress tests. Adv Compos Mater 2017:1–14
[259] Miyano Y, Nakada M, Kudoh H, Muki R. Determination of Tensile Fatigue Life of Unidirectional CFRP Specimens by Strand Testing. Mech Time-Dependent Mater 2000;4:127–37
[260] Nakada M, Miyano Y, Kinoshita M, Koga R, Okuya T, Muki R. Time–Temperature Dependence of Tensile Strength of Unidirectional CFRP. J Compos Mater 2002;36:2567–81
[261] Jeong TK, Ueda M. Longitudinal Compressive Failure of Multiple-Fiber Model Composites for a Unidirectional Carbon Fiber Reinforced Plastic. Open J Compos Mater 2016;6:8–17
[262] Jumahat A, Soutis C, Jones FR, Hodzic A. Fracture mechanisms and failure analysis of carbon fibre/toughened epoxy composites subjected to compressive loading. Compos Struct 2010;92:295–305
[263] Yokozeki T, Ogasawara T, Ishikawa T. Effects of fiber nonlinear properties on the compressive strength prediction of unidirectional carbon–fiber composites. Compos Sci Technol 2005;65:2140–7
[264] Nakanishi Y, Hana K, Hamada H. Fractography of fracture in CFRP under compressive load. Compos Sci Technol 1997;57:1139–47
[265] Thom H. A review of the biaxial strength of fibre-reinforced plastics. Compos Part A Appl Sci Manuf 1998;29:869–86
[266] Pagano NJ, Pipes RB. The Influence of Stacking Sequence on Laminate Strength. J Compos Mater 1971;5:50–7
[267] Bailey JE, Curtis PT, Parvizi A. On the Transverse Cracking and Longitudinal Splitting Behaviour of Glass and Carbon Fibre Reinforced Epoxy Cross Ply Laminates and the Effect of Poisson and Thermally Generated Strain. Proc R Soc A Math Phys Eng Sci 1979;366:599–623
[268] Wicaksono S, Chai GB. A review of advances in fatigue and life prediction of fiber-reinforced composites. Proc Inst Mech Eng Part L J Mater Des Appl 2013;227:179–95
[269] Armanios E, Bucinell R, Wilson D, Asp L, Sjogren A, Greenhalgh E. Delamination Growth and Thresholds in a Carbon/Epoxy Composite Under Fatigue Loading. J Compos Technol Res 2001;23:55
[270] Lin CT, Kao PW. Fatigue delamination growth in carbon fibre-reinforced aluminium laminates. Compos Part A Appl Sci Manuf 1996;27:9–15
[271] Gustafson C-G, Hojo M. Delamination Fatigue Crack Growth in Unidirectional Graphite/Epoxy Laminates. J Reinf Plast Compos 1987;6:36–52
[272] Dahlen C, Springer GS. Delamination Growth in Composites under Cyclic Loads. J Compos Mater 1994;28:732–81
[273] Pagano, N.J. Schoeppner, G.A. (2000). Delamination of Polymer Matrix Composites: Problems and Assessment, *Comprehensive Composite Materials*, p433-528
[274] Han Zhang, Emiliano Bilotti Ton Peijs (2015) The use of carbon nanotubes for damage sensing and structural health monitoring in laminated composites: a review, *Nanocomposites*, 1:4, 167-184
[275] Davim, J., Rubio, J., Abrao, A. (2007). A novel approach based on digital image analysis to evaluate the delamination factor after drilling composite laminates. *Composites Science and Technology*.
[276] Bak, B. L. V., Sarrado, C., Turon, A., Costa, J. (2014). Delamination Under Fatigue Loads in Composite Laminates: A Review on the Observed Phenomenology and Computational

Methods. *Applied Mechanics Reviews*.

[277] Tabiei A, Zhang W. Composite Laminate Delamination Simulation and Experiment: A Review of Recent Development. ASME. *Applied Mechanics Reviews* 2018;70(3):030801-030801-23.

[278] O Brian, T. K., Chawan, A. D., Krueger, R., Paris, I. L. (2002). Transverse tension fatigue life characterization through flexure testing of composite materials. *International Journal of Fatigue*.

[279] ASTM E647-13, 2013, Standard Test Method for Measurement of Fatigue Crack Growth Rates, *ASTM International*, West Conshohocken, PA.

[280] ASTM D6115-97, 2011, Standard Test Method for Mode I Fatigue Delamination Growth Onset of Unidirectional Fiber Reinforced Polymer Matrix Composites, *ASTM International*, West Conshohocken, PA.

[281] Robinson, P., Song, D. Q. (1994). The development of an improved mode III delamination test for composites. *Composites Science and Technology*.

[282] Hojo,M.,Ando,T.,Tanaka,M.,Adachi,T., Ochiai,S., Endo,Y., (2006) Modes I and II interlaminar fracture toughness and fatigue delamination of CF/epoxy laminates with self-same epoxy interleaf, *International Journal of Fatigue*, Volume 28, Issue 10, Pages 1154-1165.

[283] O Brien, T., Mixed-Mode Strain-Energy-Release Rate Effects on Edge Delamination of Composites, Effects of Defects in Composite Materials, STP836-EB, Wilkins, D., Ed., *ASTM International*, West Conshohocken, PA, 1984, pp. 125-142.

[284] O Brien, T., Murri, G., and Salpekar, S., Interlaminar Shear Fracture Toughness and Fatigue Thresholds for Composite Materials, Composite Materials: Fatigue and Fracture, Second Volume, STP1012-EB, Lagace, P., Ed., *ASTM International*, West Conshohocken, PA, 1989, pp. 222-250.

[285] Martin, R. and Murri, G., Characterization of Mode I and Mode II Delamination Growth and Thresholds in AS4/PEEK Composites, Composite Materials: Testing and Design (Ninth Volume), STP1059-EB, Garbo, S., Ed., *ASTM International*, West Conshohocken, PA, 1990, pp. 251-270.

[286] Tanaka, H., and Tanaka, K., 1995, Mixed-Mode Growth of Interlaminar Cracks in Carbon/Epoxy Laminates Under Cyclic Loading, *Proceedings of the 10th International Conference on Composite Materials*, Vol. 1, Whistler, Canada, pp. 181–189.

[287] Kumar SB, Sridhar I, Sivashanker S. Influence of humid environment on the performance of high strength structural carbon fiber composites. Mater Sci Eng A 2008;498:174–8

[288] Zhong Y, Joshi SC. Impact behavior and damage characteristics of hygrothermally conditioned carbon epoxy composite laminates. Mater Des 2015;65:254–64

[289] Shenoi RA, Wellicome JF. Composite materials in maritime structures Volume 1. Fundamental aspects. Cambridge University Press; 1993

[290] Broutman LJ. Fracture and Fatigue: Composite Materials. vol. 5. Academic Press, New York and London; 1974

[291] Harris B, Reiter H, Adam T, Dickson RF, Fernando G. Fatigue behaviour of carbon fibre reinforced plastics. Composites 1990;21:232–42

[292] Liotier P-J, Vautrin A, Beraud J-M. Microcracking of composites reinforced by stitched multiaxials subjected to cyclical hygrothermal loadings. Compos Part A Appl Sci Manuf 2011;42:425–37

[293] Yavuz AK, Papoulia KD, Phoenix SL, Hui CY. Stability Analysis of Stitched Composite Plate System with Delamination Under Hygrothermal Pressure. AIAA J 2006;44:1579–85

[294] Botelho EC, Pardini LC, Rezende MC. Hygrothermal effects on the shear properties of carbon fiber/epoxy composites. J Mater Sci 2006;41:7111–8

[295] Dickson RF, Jones CJ, Harris B, Leach DC, Moore DR. The environmental fatigue behaviour of carbon fibre reinforced polyether ether ketone. J Mater Sci 1985;20:60–70

[296] Jones CJ, Dickson RF, Adam T, Reiter H, Harris B. The Environmental Fatigue Behaviour of Reinforced Plastics. Proc R Soc Lond A Math Phys Sci 1984;396:315–38.

[297] Pascoe, J. A., Alderliesten, R. C., and Benedictus, R. (2013). Methods for the prediction of fatigue delamination growth in composites and adhesive bonds - A critical review. *Engineering Fracture Mechanics*, 112–113: 72–96

[298] Sevenois, R. D. B., and Van Paepegem, W. (2015). Fatigue Damage Modeling Techniques for Textile Composites: Review and Comparison With Unidirectional Composite Modeling Techniques. *Applied Mechanics Reviews*, 67: 21401

[299] Degrieck, J., and Van Paepegem, W. (2001). Fatigue damage modeling of fibre-reinforced composite materials: Review. *Applied Mechanics Reviews*, 54: 279

[300] Harris, B., Gathercole, N., Lee, J. A., Reiter, H., and Adam, T. (1997). Life-Prediction for Constant-Stress Fatigue in Carbon-Fibre Composites. *Philosophical Transactions: Mathematical, Physical and Engineering Sciences*, 355: 1259–1294

[301] Ramani S, Williams D (1076) Notched and Unnotched Fatigue Behavior of Angle-Ply Graphite/Epoxy Composites. *NASA Technical Memorandum*, 73, 191

[302] Kawai M, Matsuda Y, Yoshimura R (2012) A general method for predicting temperature-dependent anisomorphic constant fatigue life diagram for a woven fabric carbon/epoxy laminate. Composites Part A: Applied Science and Manufacturing, 43: 915–925

[303] Kawai, M., Yagihashi, Y., Hoshi, H., and Iwahori, Y. (2013). Anisomorphic constant fatigue life diagrams for quasi-isotropic woven fabric carbon/epoxy laminates under different hygrothermal environments. *Advanced Composite Materials*, 22: 79–98

[304] Whitworth, H. A. (1997). A stiffness degradation model for composite laminates under fatigue loading. *Composite Structures*, 40: 95–101

[305] Whitworth, H. A. (2000). Evaluation of the residual strength degradation in composite laminates under fatigue loading. *Composite Structures* 48: 261–264

[306] Yao, W. X., and Himmel, N. (2000). A new cumulative fatigue damage model for fibre-reinforced plastics. *Composites Science and Technology*, 60: 59–64

[307] Adam T, Gathercole N, Reiter H, Harris B. (1994) Life prediction for fatigue of T800/5245 carbon-fiber composites: II - variable-amplitude loading. *International Journal of Fatigue* 16:533-47

[308] Berardi VP, Perrella M, Feo L, Cricri G (2017) Creep behavior of GFRP laminates and their phases: Experimental investigation and analytical modelling. Composites Part B, 122, 136-144

[309] Ascione L, Berardi VP, D'Aponte A (2011) Long-term behavior of PC beams externally plated with prestressed FRP systems: A mechanical model. Composites Part B, 42, 1196-1201

[310] Berardi VP, Mancusi G (2013) A mechanical model for predicting the long term behavior of reinforced polymer concretes. Mechanics Research Communications, 50, 1-7

[311] Nedjar B (2016) Directional damage gradient modeling of fiber/matrix debonding in viscoelastic UD composites. Composite Structures, 153, 895-901

[312] Yang, Jn, Yang, Sh, and Jones, DL. (1989). A Stiffness-Based Statistical Model for Predicting the Fatigue Life of Graphite/Epoxy Laminates. *Composites Technology and Research*, 11: 129-134.

[313] Khan, Z., Al-Sulaiman, F. A., Farooqi, J. K., and Younas, M. (2001). Fatigue life predictions in woven carbon fabric/polyester composites based on modulus degradation. *Journal of Reinforced Plastics and Composites*, 20: 377–398

[314] Shokrieh, M. M., and Lessard, L. B. (2000). Progressive fatigue damage modeling of composite materials, part I: Modeling. *Journal of Composite Materials*, 34: 1056–1080

[315] Shokrieh, M. M., and Lessard, L. B. (2000). Progressive Fatigue Damage Modeling of Composite Materials, Part II: Material Characterization and Model Verification. *Journal of Composite Materials*, 34: 1081–1116

[316] Papanikos, P., Tserpes, K. I., and Pantelakis, S. (2003). Modelling of fatigue damage progression and life of CFRP laminates.

Fatigue and Fracture of Engineering Materials and Structures, 26: 37–47

[317] Kennedy, C. R., Ó Brádaigh CM, Leen, S. B. (2013). A multiaxial fatigue damage model for fibre reinforced polymer composites. Composite Structures, 106: 201-210

[318] Puck, A., Schurmann, H. (2002). Failure analysis of FRP laminates by means of physically based phenomenological models. Composites Science and Technology, 62: 1633-1662

[319] Puck, A., Kopp, J., Knops, M. (2002). Guidelines for the determination of the parameters in Puck's action plane strength criterion. Composites Science and Technology, 62: 371-378

[320] Lin Ye. (1988). Role of matrix resin in delamination onset and growth in composite laminates. *Composites Science and Technology*, 33: 257–277

[321] Harper, P. W., and Hallett, S. R. (2010). A fatigue degradation law for cohesive interface elements - Development and application to composite materials. *International Journal of Fatigue*, 32: 1774–1787

[322] Tserpes, K. I., Labeas, G., Papanikos, P. Kermanidis, T. (2002). Strength prediction of bolted joints in graphite/epoxy composite laminates. *Composites Part B: Engineering*, 33: 521–529

[323] Blanco, N., Gamstedt, E. K., Asp, L. E., and Costa, J. (2004). Mixed-mode delamination growth in carbon-fibre composite laminates under cyclic loading. *International Journal of Solids and Structures*, 41: 4219–4235

[324] May, M., and Hallett, S. R. (2010). A combined model for initiation and propagation of damage under fatigue loading for cohesive interface elements. *Composites Part A: Applied Science and Manufacturing*, 41: 1787–1796

[325] Allegri, G., Jones, M. I., Wisnom, M. R., and Hallett, S. R. (2011). A new semi-empirical model for stress ratio effect on mode II fatigue delamination growth. *Composites Part A: Applied Science and Manufacturing*, 42: 733–740

[326] Allegri, G., Wisnom, M. R., and Hallett, S. R. (2013). A new semi-empirical law for variable stress-ratio and mixed-mode fatigue delamination growth. *Composites Part A: Applied Science and Manufacturing*, 48: 192–200

[327] Kawashita, L. F., and Hallett, S. R. (2012). A crack tip tracking algorithm for cohesive interface element analysis of fatigue delamination propagation in composite materials. *International Journal of Solids and Structures*, 49: 2898–2913

[328] Tao, C., Qiu, J., Yao, W., and Ji, H. (2016). A novel method for fatigue delamination simulation in composite laminates. *Composites Science and Technology*, 128: 104–115

[329] Talreja, R . (1996) A synergistic Damage Mechanics Approach to Durability of Composite Material Systems. *Progress in Durability Analysis of Composite Systems*, Cardon, Fukuda and Reifsnider, Eds., Balkema, Rotterdam, 117-129

[330] Talreja, R. (1985). A Continuum Mechanics Characterization of Damage in Composite Materials. *Proceedings of the Royal Society A: Mathematical, Physical and Engineering Sciences*, 399: 195–216

[331] Talreja, R. (1990) Internal Variable Damage Mechanics of Composite Materials, Yielding, Damage and Failure of Anisotropic Solids, EGF5, Mechanical Engineering Publications, London, 1991, pp. 509-553

[332] Talreja, R. (2008). Damage and fatigue in composites - A personal account. Composites Science and Technology, 68: 2585–2591

[333] Singh, C. V., and Talreja, R. (2009). A synergistic damage mechanics approach for composite laminates with matrix cracks in multiple orientations. *Mechanics of Materials*, 41: 954–968

[334] Singh, C. V., and Talreja, R. (2010). Evolution of ply cracks in multidirectional composite laminates. *International Journal of Solids and Structures*, 47: 1338–1349

[335] Montesano, J., and Singh, C. V. (2015). Predicting evolution of ply cracks in composite laminates subjected to biaxial loading. *Composites Part B: Engineering*, 75: 264–273

[336] Haojie, S., Weixing, Y., Yitao, W. (2014). Synergistic damage mechanic model for stiffness properties of early fatigue damage in composite laminates. *Procedia Engineering* 74: 199–209